Hindawi
Geofluids
Volume 2022, Article ID 2177030, 21 pages
https://doi.org/10.1155/2022/2177030

Research Article

The Effect of Tectonic Stress and Thermal Evolution on Shale Pores of Devonian and Carboniferous Shales in Southern China

Zhiyao Zhang,[1] **Shang Xu**,[2] **Wanzhong Shi**,[1] **Fanyang Meng**,[3] **Qiyang Gou**,[1] **and Mingfang Zhao**[1]

[1]*Key Laboratory of Tectonics and Petroleum Resources, Ministry of Education, China University of Geosciences, Wuhan 430074, China*
[2]*Shandong Provincial Key Laboratory of Deep Oil& Gas, University of Petroleum (East China), Qingdao 266580, China*
[3]*Oil and Gas Survey, China Geological Survey, Beisihuan Road No. 267, Haidian District, Beijing 100083, China*

Correspondence should be addressed to Shang Xu; xushang0222@163.com

Received 15 February 2022; Revised 23 April 2022; Accepted 8 May 2022; Published 8 June 2022

Academic Editor: Mohammed Fattah

Many sets of Paleozoic marine organic-rich shale strata are developed in southern China. However, the exploration and development degree of these strata are different. Cambrian shale and Ordovician-Silurian shale are two horizons with high degree of exploration, while Devonian shale and Carboniferous shale exploration is deficient. Based on XRD, FE-SEM, and gas adsorption experiment, pore development characteristics and controlling factors of Devonian and Carboniferous shale are investigated. There are mainly four lithofacies in Devonian and Carboniferous shale: mixed shale (M), carbonate/siliceous mixed shale (M-1), argillaceous/siliceous mixed shale (M-2), and argillaceous-rich siliceous shale (S-3). Reservoir characteristics of both two sets of shale strata are quite different. The averages of porosity, pore volume, and specific surface area of Devonian shale are 3.81%, 9.7×10^{-3} cm^3/g and 11.8 m^2/g, while those of Carboniferous shale are 3.57%, 17.3×10^{-3} cm^3/g and 19.8 m^2/g. Thermal evolution (Ro) and tectonic preservation conditions are the main factors affecting the pore development. Carboniferous shale ($Ro \approx 2\%$) is in the stage of producing a large number of organic pores. Devonian shale ($Ro \approx 3.5\%$) is having difficulty preserving organic pores due to high thermal evolution. Meanwhile, Devonian shale (well GTD1) is strongly affected by tectonic movement; tectonic fractures and calcite veins are developed. Carboniferous shale (well GRY1) is in relatively stable area; tectonic fractures are not developed. Under the influence of compaction, the pore volume and specific surface area of Carboniferous shale are 78.3% and 67.8% higher than those of Devonian shale, respectively. This research can provide reference for clarifying shale pore development and evolution mechanism and similar shale gas exploration both in study area and around the world.

1. Introduction

Due to the horizontal drilling and hydraulic fracturing, shale gas exploration and development in the United States have been relatively successful and energy independence has been realized. The main gas-producing shales in the United States are Devonian shale, Carboniferous shale, and Permian shale, such as Devonian Marcellus shale in Appalachian Basin, Devonian Woodford shale in Anadarko Basin, Carboniferous Barnett shale in Fort Worth Basin, Carboniferous Fayetteville shale in Arkoma Basin, and Permian Wolfcamp shale in Midland Basin [1–5]. Gas-producing shales in the United States have relatively new stratigraphic age, low thermal evolution, low hydrocarbon expulsion efficiency, and better preservation conditions [6–8]. After the United States and Canada, China has also taken the lead in realizing the commercial exploitation of shale gas. China mainly makes breakthroughs in ancient shales, such as Silurian Longmaxi shale in Sichuan Basin, Cambrian Niutitang shale in Western Hubei, and Ordovician Wulalike shale in Erdos Basin [9–13]. The exploration and development of Late Paleozoic Devonian-Carboniferous organic-rich shale widely developed in South China are still in the early stage. Therefore,

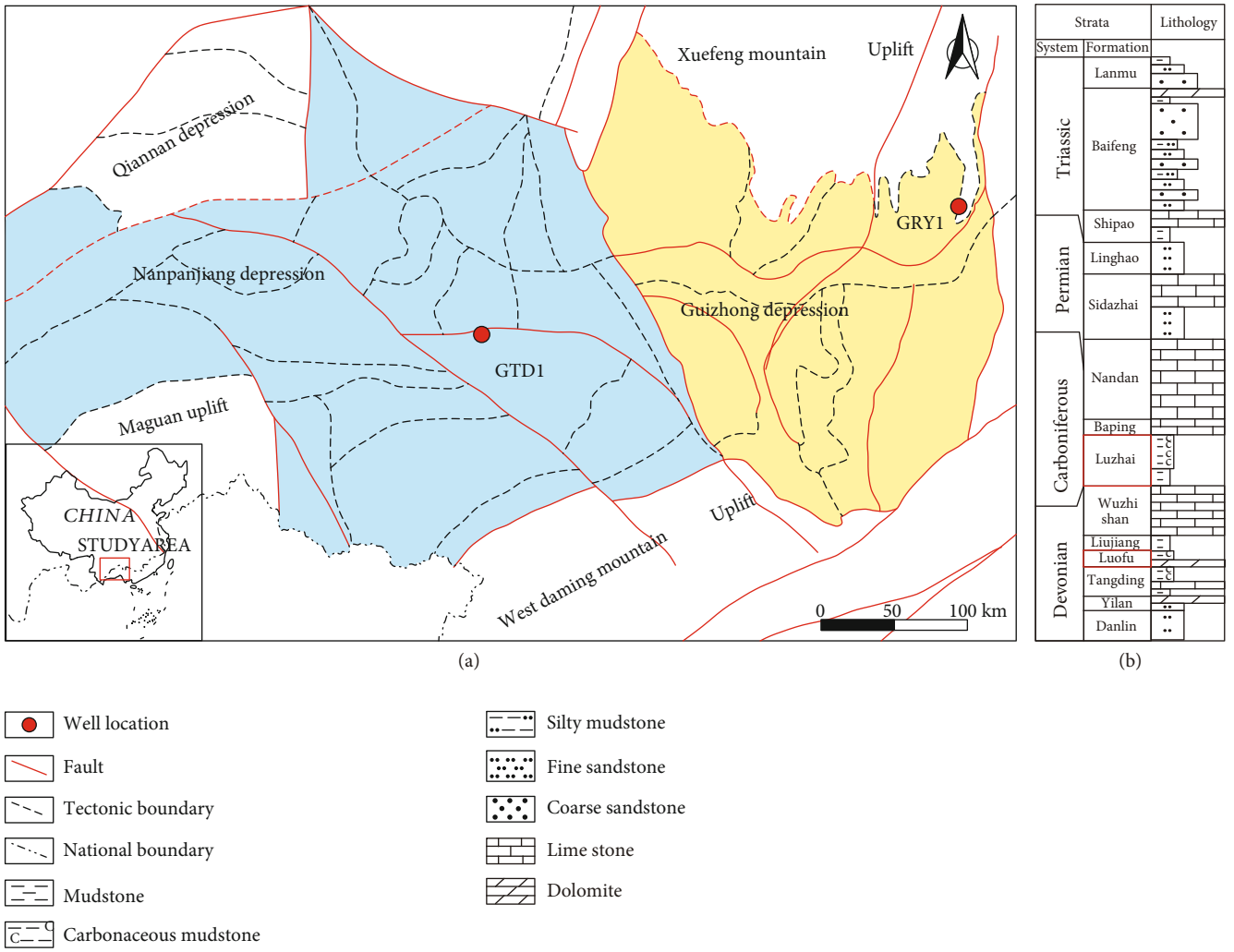

Figure 1: (a) The location of study area; (b) stratigraphic histogram of the study area.

it is necessary to further evaluate the characteristics and gas-bearing property of Devonian and Carboniferous organic-rich shale reservoirs.

Studies on the pores of shale reservoir have had a relatively comprehensive understanding, including type, morphology, volume and specific surface area, connectivity, and roundness [10–22]. Previous studies have shown that there are many factors affecting the pore development of shale reservoir [21–24]. A large number of siliceous mineral particles in siliceous shale can better prevent the destruction of primary pores, better preserve reservoir space, and play a positive role in the enrichment of shale gas [25–32]. When the Ro is greater than 2%, a large number of organic pores begin to develop in organic matter, while when Ro is less than 0.5%, the organic pores are basically not developed [24]. The formation pressure in the tectonic stable area is well preserved, and the reservoir has strong support capacity, which can offset the compaction of the overlying strata and is conducive to the preservation of pores. However, due to the release of formation pressure, the pores are usually destroyed under the compaction of the overlying strata in the tectonic deformation area [33–36].

The investigated samples were collected from two wells (well GRY1 and well GTD1) for comparative analysis of pore developmental characteristics and controlling factors of Devonian and Carboniferous shales (Figure 1). The main purposes are as follows: (1) investigating the petrological and mineralogical characteristics and lithofacies development characteristics of Devonian and Carboniferous organic-rich shale and (2) analyzing the pore structure characteristics and controlling factors of Devonian and Carboniferous organic-rich shale in southern China.

2. Geological Setting

In this paper, the study area includes southern Guizhou Province, central and Western Guangxi Province, and eastern Yunnan Province, which is in the tectonic transformation area under the joint action of Pacific tectonic domain and Tethys tectonic domain (Figure 1(a)). It is a passive continental margin rift basin formed by the return of southern China fold system caused by Guangxi movement at the end of Early Paleozoic. In the Triassic, it evolved into a

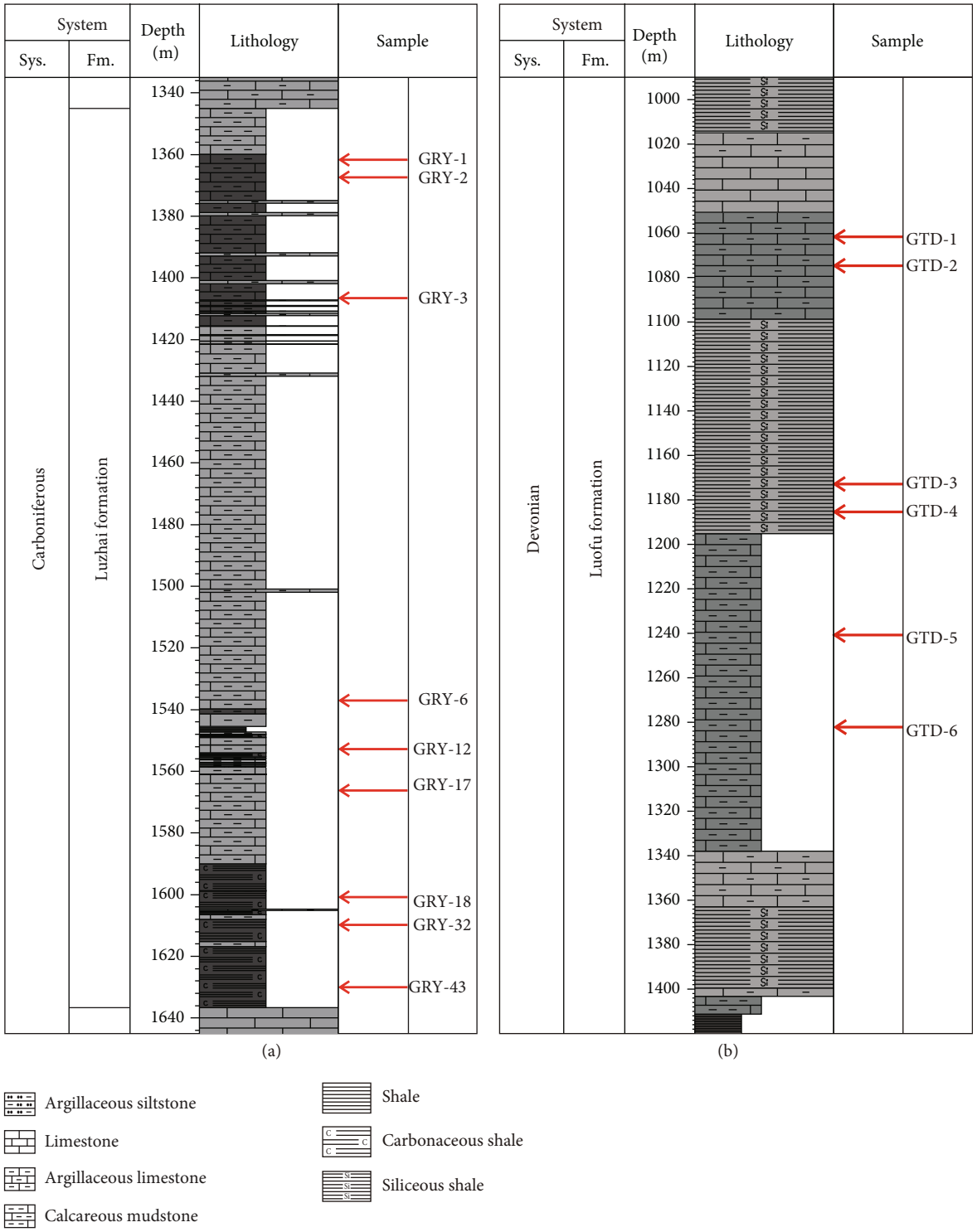

Figure 2: (a) Lithology and sampling location in well GRY1; (b) lithology and sampling location in well GTD1.

unified turbidite basin, and the sedimentary filling process is complicated [37, 38].

The study area is located in the southern margin of the Caledonian Yangtze ancient plate and the northwest of the South China magmatic orogenic belt. It is bounded by Guiyang-Zhenyuan fault, Wuling depression, and central Guizhou Uplift in the north; Xuefeng mountain uplift (Jiangnan ancient land) in the northeast; Longsheng-Yongfu fault, Dayaoshan fault, Guilin depression, and Dayaoshan uplift in the East; and Maguan uplift in the West. Three primary depressions are mainly developed in the basin, namely, Qiannan depression, Guizhong depression, and Nanpanjiang depression; multiple secondary depressions are developed in these primary depressions [39–41]. This area has experienced multistage tectonic movements such as Caledonian, Hercynian, and Indosinian. Generally, it is characterized by first uplift

Table 1: TOC, mineral composition, and lithofacies of shale samples in GRY1 and GTD1.

Well	Sample ID	Mineral composition					TOC (Wt.%)	Porosity (%)	Lithofacies
		Quartz (%)	Feldspar (%)	Carbonate (%)	Pyrite (%)	Clay (%)			
GRY1	GRY-1	42.8	1.3	32.4	1	21.9	0.36	3.66	M-1
	GRY-2	46.1	1.2	25.3	1.2	25.8	1.42	3.12	M-3
	GRY-3	54.7	1.7	10.6	1.7	30.8	1.2	4.35	S-3
	GRY-6	54.8	1.4	13.9	1.2	28.3	1.55	3.52	S-3
	GRY-12	45.7	1.7	18.1	1.3	32.9	1.04	3.38	M-2
	GRY-17	50.1	1.3	15.6	0.9	31.5	1.22	3.65	S-3
	GRY-18	45.1	2	7.7	2.5	41.1	1.73	4.97	M-2
	GRY-32	43.2	2.4	17	1.7	34.5	2.21	4.09	M-2
	GRY-43	42.6	1.7	24.8	1.7	28.5	2.14	3.51	M-3
GTD1	GTD-1	36.3	2	40.3	1.5	18.2	—	4.43	M-1
	GTD-2	35.0	1.8	37.4	1.4	23	1.24	3.47	M-1
	GTD-3	49.9	4.1	4.9	0.6	37.4	0.591	5.06	S-3
	GTD-4	58.8	3.3	0.5	0.4	36	0.481	2.14	S-3
	GTD-5	47.6	3.4	9.1	0.9	38.2	0.86	3.49	S-3
	GTD-6	50.0	3	4.6	0.7	40.4	0.598	2.87	S-3

and then subsidence. Specifically, after Caledonian uplift and denudation, it was affected by marine transgression from Early Devonian to Middle Triassic, and marine sedimentary strata such as Devonian, Carboniferous, and Permian were developed on the Cambrian basement (Figure 1(b)) [37, 38].

The sedimentation of the Lower Carboniferous Luzhai shale most likely occurred in low-energy anoxic platform-margin to open-platform environment [33, 42]; the deposition thickness is about 300 m. The sedimentary environment of the Middle Devonian Luofu shale is similar to that of the Luzhai shale [43]. Deposition thickness (about 420 m) is slightly greater than Luzhai shale. Both two sets of shale belong to the potential intervals for shale gas exploration and development in southern China.

3. Samples and Methodology

The investigated shale samples were obtained from well GRY1 and well GTD1, including 9 samples from Carboniferous shales in well GRY1, and 6 samples were from Devonian shales in well GTD1 (Figures 2(a) and 2(b)). Shale samples were analyzed by scanning electron microscopy (FE-SEM), CO_2 adsorption, and N_2 adsorption. Table 1 lists the measured results of TOC content (Wt.%), XRD mineralogy (Wt.%), and helium porosity of shale samples. The TOC of Carboniferous and Devonian shale are about 1.43% and 0.75%, respectively. And the helium porosity of Carboniferous and Devonian cylindrical (about 2.5 cm diameter) shale samples is about 3.8% and 3.57%.

3.1. Field Emission Scanning Electron Microscopy (FE-SEM). In order to observe the pore type, morphology, number, and microfracture development of shale in details, the combination of argon ion milling and field emission scanning electron microscopy (FE-SEM) was used to observe the Devonian and Carboniferous shale samples in the studied area [44, 45].

The preparation of shale samples for field emission scanning electron microscopy analysis is divided into the following steps: (1) one surface with an area of about 1 cm^3 and a thickness of no more than 0.8 cm is selected; (2) Leica EM XTP produced by Leica company in the United States is selected for the first milling; and (3) Leica EM RES102 is selected for the second milling. The experimental conditions are as follows: acceleration voltage of 5 kV, gun current of about 2 mA, time of 2 h, and ion beam angle of 2.5°. After that, the prepared shale samples were placed under the field emission scanning electron microscope, and the Zeiss Merlin compact system was used for fine observation. In this paper, the experimental conditions are as follows: working voltage of 2 kV and working distance 4-6 mm.

3.2. Low-Pressure Gas Isothermal Adsorption. For characterizing the pore structure in shale reservoir in details, low-pressure gas adsorption (CO_2 adsorption and N_2 adsorption) is a routine method. Through the measurement of N_2 and CO_2 adsorption capacity in shale pores under different pressure conditions, combined with the pore volume of each pore size under different models, the pore distribution in shale reservoirs can be characterized [15, 32].

In order to obtain information about shale micropores, Autosorb IQ MP analyzer produced by Quantachrome Company in the United States was chosen to carry out CO_2 adsorption experiments on Devonian and Carboniferous shale samples. Before the experiment was operated, the shale samples were crushed into 60-80-mesh particles and degassed in a vacuum at 383 K for about 14 hours to eliminate the effects of volatile substances and adsorbed water [11]. The CO_2 isothermal adsorption curve was carried out at 273.15 K (ice water bath), the relative pressure (P/P_0) was 4×10^{-4}-3×10^{-2}, the equilibrium interval is 30 s, and the shale micropore distribution is calculated according to the DFT model [15, 31].

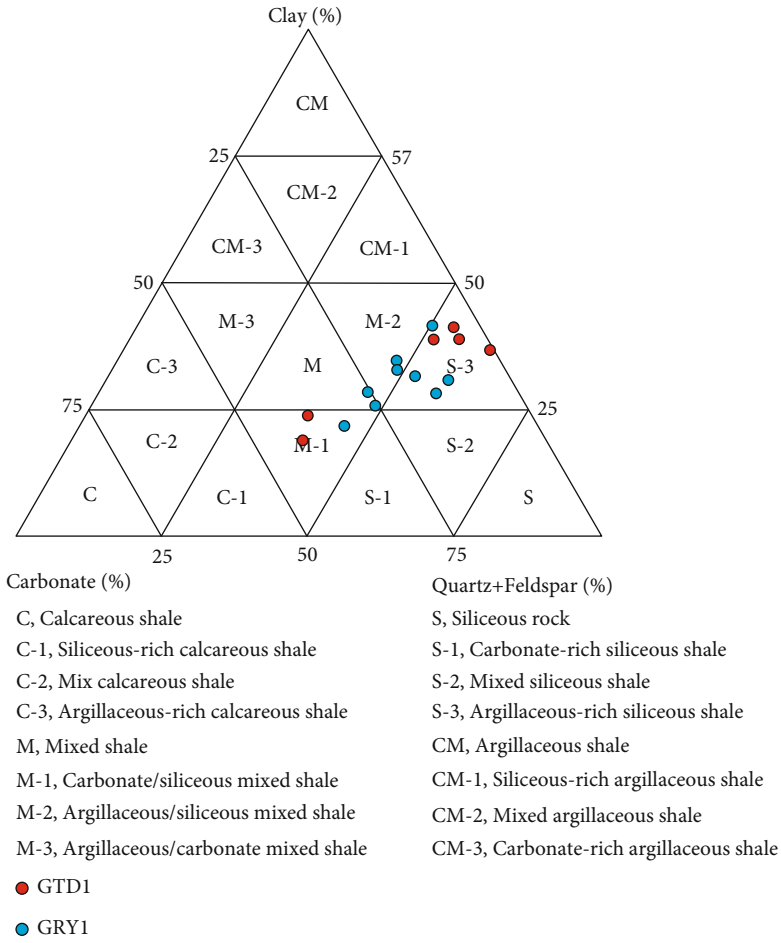

Figure 3: Ternary diagram of mineral compositions of shale samples in well GRY1 and well GTD1.

For the purpose of obtaining the information about mesopores and macropores of shale, Micromeritics ASAP 2020 Surface Area and Porosity Analyzer produced by Micromeritics instrument Company in the United States was selected to analyze Devonian and Carboniferous shale samples for N_2 adsorption experiments. The adsorption and desorption of N_2 in shale samples were measured under the conditions of temperature 77.35 K, relative pressure range 0.005-1.0, and equilibrium interval 30 s. The distribution of mesopores and macropores in shale is calculated according to BJH model [15, 31, 32, 46].

4. Results

4.1. Mineral Composition and Lithofacies Classification. In this study, 15 typical representative shale samples from two wells were selected for XRD test. Experimental data shows that the shales of Devonian Luofu formation in well GTD1 and Carboniferous Luzhai formation in well GRY1 have similar mineral composition, mainly quartz, feldspar, pyrite, clay minerals, and carbonate minerals, in which the content of siliceous minerals (quartz and feldspar) is high, and the content of carbonate minerals is relatively low. The siliceous mineral content of Luzhai formation shale is 42.6%-54.8% (average 47.23%); the carbonate mineral content is 7.7%-32.4% (average 18.7%); and the clay mineral content is 21.9%-41.1% (average 30.6%). And the siliceous mineral content of Luofu shale is 31.8%-73.2% (average of 48.94%); the carbonate mineral content is 0.5%-40.3% (average 16.1%); and the clay mineral content is 18.2%-40.4% (average 32.2%).

According to the X-ray diffraction of in Devonian and Carboniferous shale Table 1, four lithofacies are classified in lithofacies triangle diagram [47, 48], including mixed shale (M), carbonate/siliceous mixed shale (M-1), argillaceous/siliceous mixed shale (M-2), and argillaceous-rich siliceous shale (S-3). Middle Devonian Luofu shale develops two lithofacies types: lime-rich mixed shale and mud-rich siliceous shale. Lower Carboniferous Luzhai shale develops four lithofacies types: lime-rich mixed shale, mud-rich mixed shale, mixed shale, and mud-rich siliceous shale (Figure 3).

4.2. SEM Pore Characteristics. According to the results of SEM, the pore types in Devonian and Carboniferous shale samples in the study area mainly include organic pores, inorganic pores, and microfractures (Figure 4).

Organic pore is one of the main pore types in shale samples, which are widely distributed in areas containing organic matter [24, 26, 29, 30]. The organic pores of

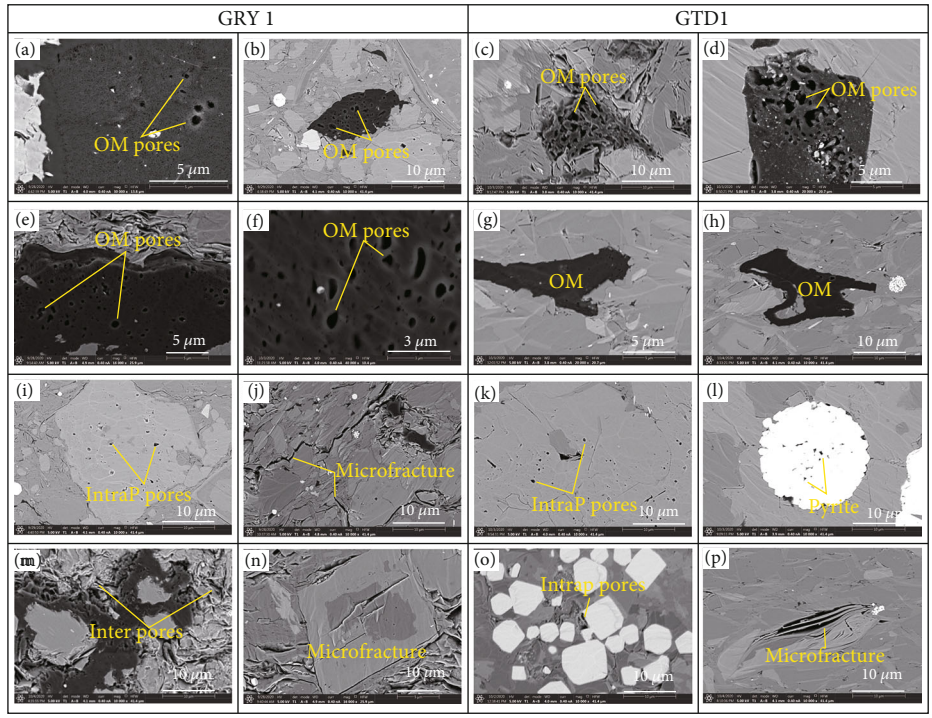

Figure 4: SEM photos of shale samples in well GRY1 and well GTD1: (a) round-oval organic pores, 1361.7 m, well GRY1; (b) round-oval organic pores, 1367.4 m, well GRY1; (c) collapse-closure organic pores, 1050.0 m, well GTD1; (d) collapse-closure organic pores, 1050.0 m, well GTD1; (e) round-oval organic pores, 1599.3 m, well GRY1; (f) round-oval organic pores, 1534.8 m, well GRY1; (g) irregular organic matter, 1178.4 m, well GTD1; (h) irregular organic matter, 1235.9 m, well GTD1; (i) intragranular pore, 1367.4 m, well GRY1; (j) microfractures, 1628.3 m, well GRY1; (k) intragranular pore, 1050.0 m, well GTD1; (l) pyrite framboids, 1050.0 m, well GTD1; (m) intergranular pore, 1552.7 m, well GRY1; (n) microfractures, 1599.3 m, well GRY1; (o) intergranular pore, 1165.5 m, well GTD1; (p) microfractures, 1235.9 m, well GTD1.

Carboniferous shale are relatively developed. Most of the organic pores are round oval, and a few are slit or strip (Figures 4(a), 4(b), 4(e), and 4(f)). There are few organic pores in Devonian shale, and those that developed organic pores only show the characteristics of collapse and closure (Figures 4(c), 4(d), 4(g), and 4(h)).

Inorganic pores and microfractures are also important pore types in Devonian and Carboniferous shale samples. Inorganic pores can be divided into intergranular pores and intragranular pores. Intergranular pores are generally distributed between rigid particles such as quartz, feldspar, and calcite or flaky clay minerals. They are generally triangular and polygonal, with straight edges and relatively large sizes ranging from nano- to several microns (Figures 4(l), 4(m), and 4(o)). The formation of intragranular pores is related to the dissolution of mineral particles, and the size is small, generally tens of nanometers (Figures 4(i) and 4(k)). Microfracture formed by the fracture of particles in shale due to tectonic movement or compaction. They are generally distributed in the interior or edge of mineral particles, and the length does not exceed 50 microns (Figures 4(j), 4(n), and 4(p)).

4.3. Quantitative Analysis of Pore Structures. According to the pore classification standard of IUPAC, it is proposed to divide the nanopores of shale into micropores (pore diameter < 2 nm), mesopores (pore diameter 2-50 nm), and macropores (pore diameter > 50 nm). Since carbon dioxide gas can enter pores with a diameter of 0.35 nm, the micropore distribution can be calculated by the DFT model. According to the BJH model, N_2 adsorption can effectively characterize the pore volume and specific surface area of mesopores and macropores by measuring the liquid N_2 content in pores under different pressure conditions. Therefore, the micropores of shale reservoirs of Lower Carboniferous Luzhai shale (well GRY1) and Middle Devonian Luofu shale (well GTD1) can be characterized by low-temperature CO_2 adsorption and N_2 adsorption/desorption.

4.3.1. Analysis of CO_2 Adsorption. The CO_2 adsorption curves of 9 samples in well GRY1 are shown in Figure 5(a). The adsorption capacity of mud-rich mixed shale is the largest, with an average of 1.4 cm^3/g, followed by mixed shale and lime-rich mixed shale, with an average of 1.0 cm^3/g and 0.9 cm^3/g, respectively, and the adsorption capacity of mud-rich siliceous shale is the smallest, with an average of 0.8 cm^3/g. The CO_2 adsorption curves of 6 samples in well GTD1 are shown in Figure 5(b). The adsorption capacity of lime-rich mixed shale is large, with an average of 0.7 cm^3/g, and that of mud rich siliceous shale is small, with an average of 0.6 cm^3/g.

At the same time, based on the DFT model, we recognize that the pore size distribution of micropores in Devonian and Carboniferous shale presents the characteristics of multiple peaks in the range of 0.3-1.0 nm, indicating that these pores have a large pore volume (Figures 5(c) and 5(d)).

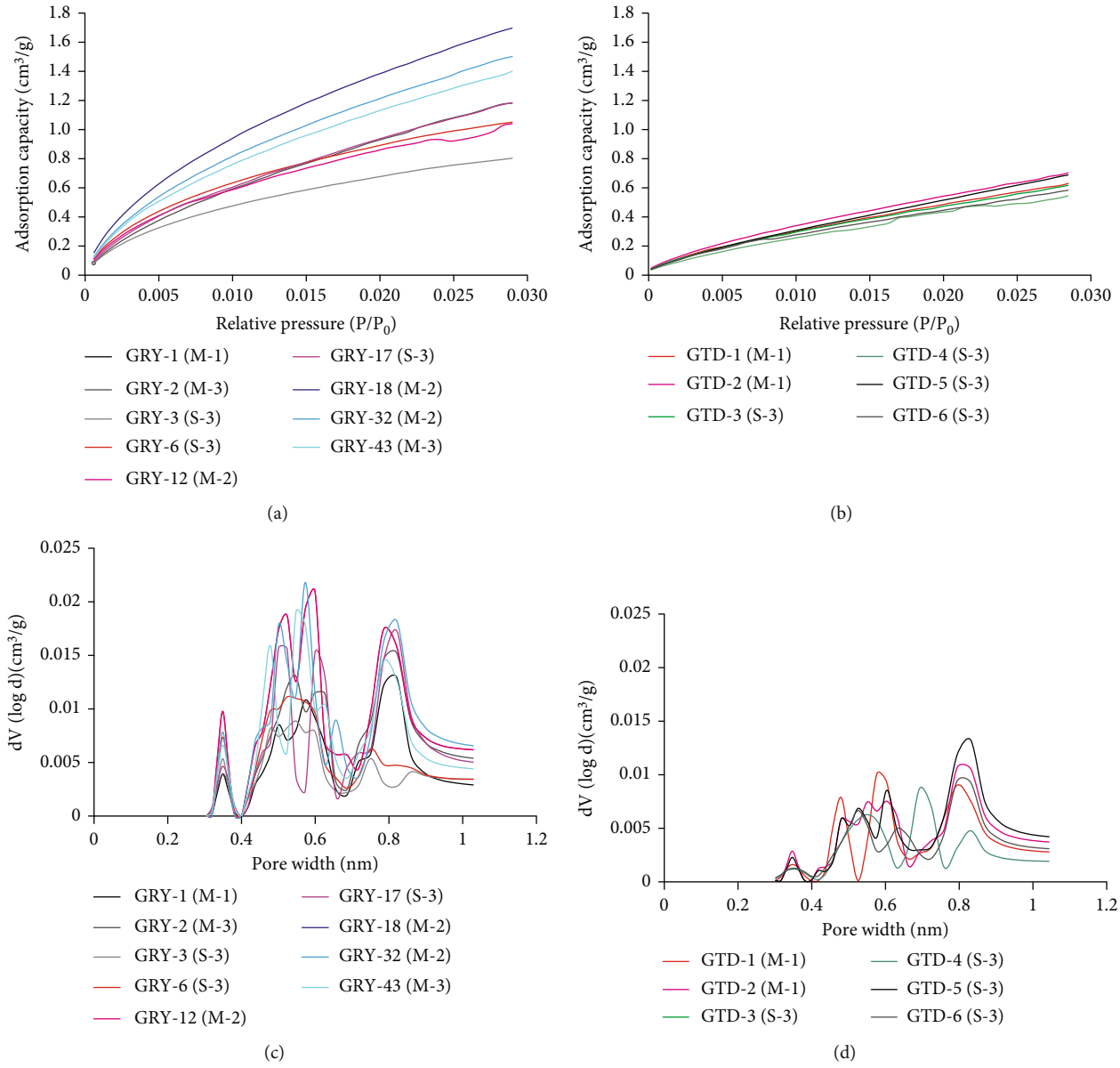

Figure 5: (a) CO_2 adsorption curve of Carboniferous shale samples in well GRY1; (b) CO_2 adsorption curve of Devonian shale samples in well GTD1; (c) CO_2 pore diameter distribution curve of Carboniferous shale samples in well GRY1; (d) CO_2 pore diameter distribution curve of Devonian shale samples in well GTD1.

4.3.2. Analysis of N_2 Adsorption. The hysteresis loops formed by N_2 adsorption/desorption curves of all shale samples from well GRY1 and well GTD1 are H3 and H4, indicating that the pore types are mainly plate pores and slit pores [15].

The N_2 adsorption curves of 9 shale samples from well GRY1 show that the distribution range of maximum N_2 adsorption capacity is 8 cm^3/g-12 cm^3/g (Figure 6(a)). And there are great differences in N_2 adsorption characteristics among different lithofacies. The adsorption capacity of mud-rich mixed shale is the largest, with an average of 10.5 cm^3/g, followed by mixed shale and mud-rich siliceous shale, with an average of 8.6 cm^3/g and 8.26 cm^3/g, respectively. The adsorption capacity of lime-rich mixed shale is the smallest, with an average of 6.1 cm^3/g. The N_2 adsorption curves of 6 shale samples from well GTD1 are shown in the figure, and the distribution range of maximum N_2 adsorption capacity is 4 cm^3/g-6 cm^3/g (Figure 6(b)). There is no obvious difference in N_2 adsorption characteristics between different lithofacies. The lime-rich mixed shale (average 6 cm^3/g) is slightly larger than the mud-rich siliceous shale (average 5 cm^3/g).

In addition, based on the BJH model and N_2 adsorption, it is recognized that the Devonian and Carboniferous shales have similar pore size distribution characteristics, but the pore volume in each pore size interval is different (Figures 6(c) and 6(d)).

4.3.3. Characterization of Total Pore Diameter. In order to comprehensively characterize the pore characteristics of shale reservoir, the pores characterized by CO_2 and N_2 adsorption are spliced to obtain the full pore size

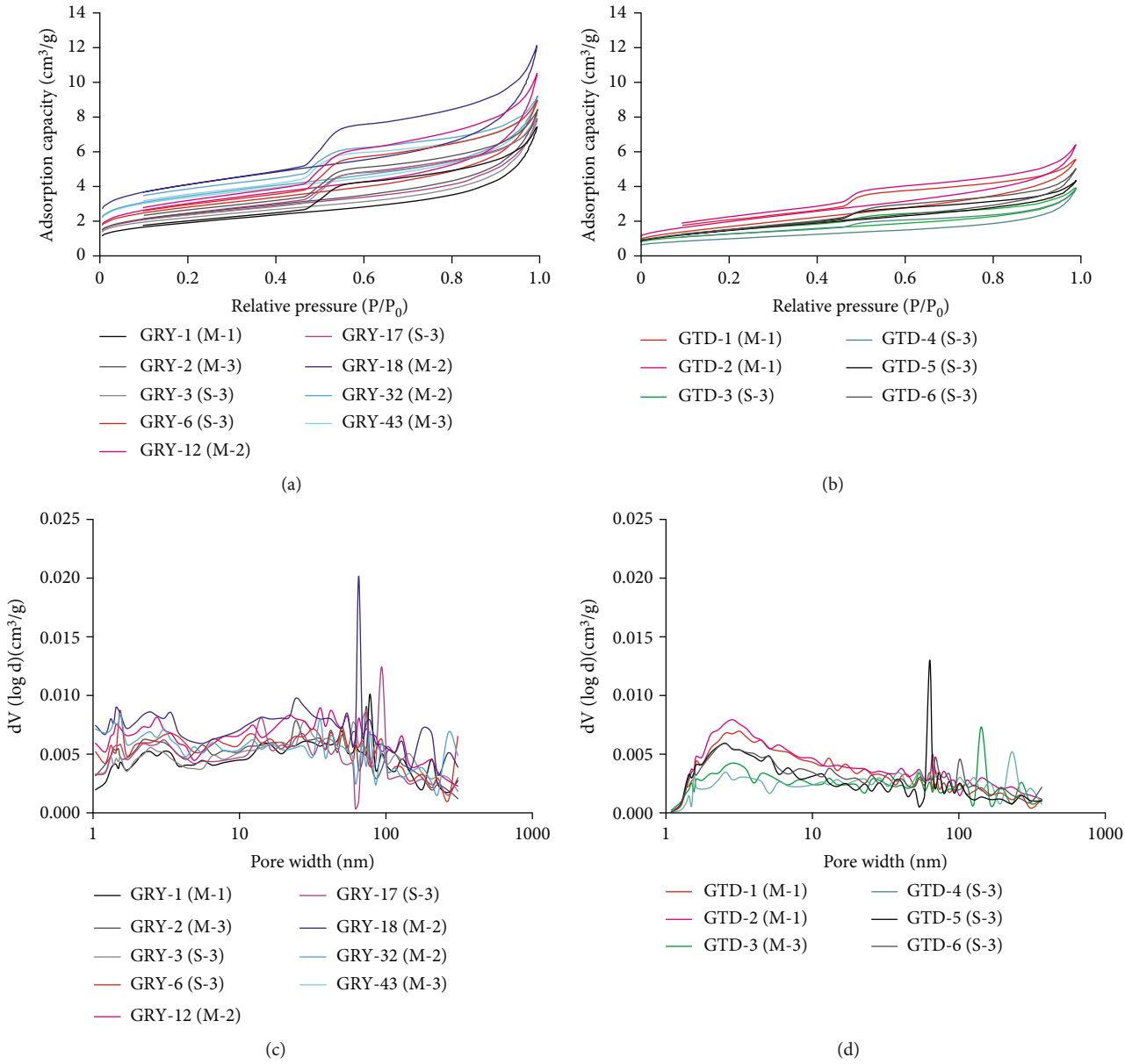

FIGURE 6: (a) N_2 adsorption curve of Carboniferous shale samples in well GRY1; (b) N_2 adsorption curve of Devonian shale samples in well GTD1; (c) N_2 pore diameter distribution curve of Carboniferous shale samples in well GRY1; (d) N_2 pore diameter distribution curve of Devonian shale samples in well GTD1.

distribution characteristics of Devonian shale and Carboniferous shale.

Figure 7(a) shows that the full pore size distribution range of Carboniferous shale is 0.3-400 nm, the peak pore size of micropores is 0.6-0.8 nm, and the peak pore size of macropores is mainly 60-80 nm; there is no obvious difference in pore size distribution between different lithofacies. Analysis shows that the total pore volume of Carboniferous shale is mainly 14.3×10^{-3} cm^3/g-21.7×10^{-3} cm^3/g, with an average of 17.3×10^{-3} cm^3/g; the micropore volume is between 3.3×10^{-3} cm^3/g and 10.0×10^{-3} cm^3/g, with an average of 5.7×10^{-3} cm^3/g; the mesopore volume is between 7.2×10^{-3} cm^3/g and 10.5×10^{-3} cm^3/g, with an average 8.3 $\times 10^{-3}$ cm^3/g; and the macropore volume is between 2.8×10^{-3} cm^3/g and 4.3×10^{-3} cm^3/g, with an average of 3.4×10^{-3} cm^3/g. The total specific surface area is mainly between 14.1 m^2/g and 26.8 m^2/g, with an average of 19.8 m^2/g. The micropore specific surface area is between 9.9 m^2/g and 20.5 m^2/g, with an average of 14.9 m^2/g; the mesopore specific surface area is between 3.8 m^2/g and 6.1 m^2/g, with an average of 4.8 m^2/g; and the macropore specific surface area is between 0.12 m^2/g and 0.18 m^2/g, with an average of 0.14 m^2/g. Analysis shows that the pore volume and specific surface area of Carboniferous shale are mainly provided by micropores and mesopores. The pore volume and specific surface area of micropores and mesopores account for about

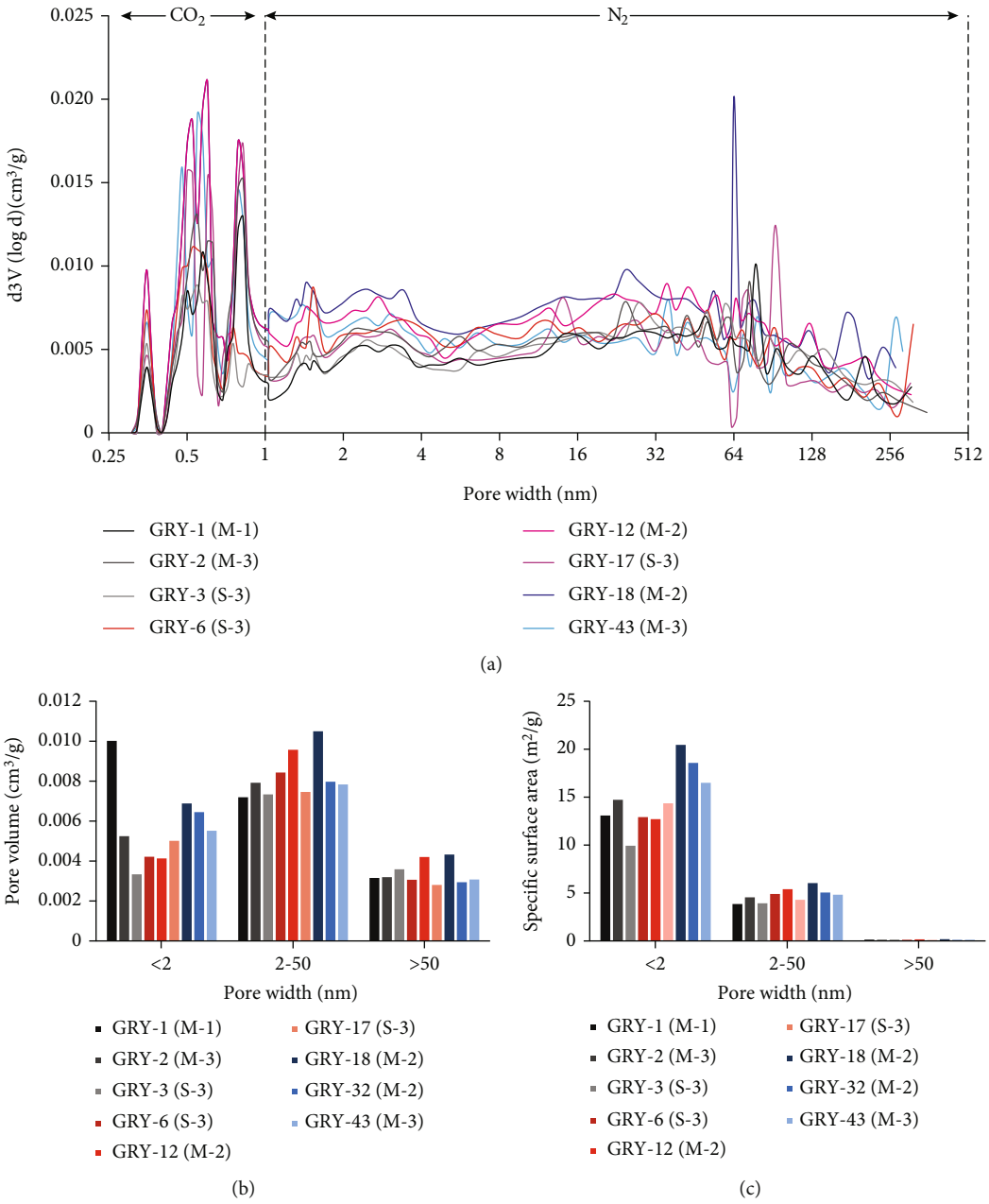

Figure 7: (a) N_2 and CO_2 pore diameter adsorption curve of Carboniferous shale samples in well GRY1; (b) pore volume distribution of Carboniferous shale samples in well GRY1; (c) pore specific surface area of Carboniferous shale samples in well GRY1.

80% of the total pore volume and 90% of the total specific surface area, respectively (Table 2, Figures 7(b) and 7(c)).

Figure 8(a) shows that the Devonian shale has peaks in the range of micropores, mesopores, and macropores, with distribution ranges of 0.5-0.8 nm, 2-4 nm, and 60-80 nm, respectively. The peak values of different lithofacies are different, and the lime-rich mixed shale is slightly larger than the mud-rich siliceous shale. The pore volume of Devonian shale is mainly 7.4×10^{-3} cm^3/g-12.3×10^{-3} cm^3/g, with an average of 9.7×10^{-3} cm^3/g; micropore volume between 2.1×10^{-3} cm^3/g and 3.5×10^{-3} cm^3/g, with an average of 3.1×10^{-3} cm^3/g; mesopore volume between 3.6×10^{-3} cm^3/g and 6.8×10^{-3} cm^3/g, with an average of 5.0×10^{-3} cm^3/g; and macropore volume between 1.3×10^{-3} cm^3/g and 2.0×10^{-3} cm^3/g, with an average of 1.6×10^{-3} cm^3/g. The specific surface area is mainly between 8.2 m^2/g and 14.4 m^2/g, with an average of 11.8 m^2/g. The micropore specific surface area is between 6.0 m^2/g and 9.4 m^2/g, with an average of 8.2 m^2/g; the mesopore specific surface area is between 2.2 m^2/g and 4.9 m^2/g, with an average of 3.6 m^2/g; and the macropore specific surface area is between 0.05 m^2/g and 0.08 m^2/g, with an average of 0.06 m^2/g. The pore volume and specific surface area of Devonian shale are also mainly provided by micropores and mesopores. Pore volume and specific

Table 2: Volumes and specific surface areas of micropores, mesopores, and macropores of shale samples in GRY1 and GTD1.

Well	Sample ID	Volume (10^{-3} cm^3/g)				Specific surface area (m^2/g)				Lithofacies
		Micropore	Mesopore	Macropore	Total	Micropore	Mesopore	Macropore	Total	
GRY1	GRY-1	10.029	7.204	3.155	20.389	13.153	3.870	0.135	17.159	M-1
	GRY-2	5.253	7.929	3.198	16.380	14.787	4.570	0.133	19.489	M-3
	GRY-3	3.337	7.346	3.588	14.270	9.982	3.957	0.149	14.087	S-3
	GRY-6	4.221	8.443	3.062	15.726	12.982	4.923	0.132	18.036	S-3
	GRY-12	4.133	9.584	4.205	17.922	12.762	5.427	0.177	18.366	M-2
	GRY-17	5.019	7.466	2.806	15.291	14.431	4.318	0.115	18.863	S-3
	GRY-18	6.891	10.508	4.328	21.727	20.546	6.071	0.183	26.800	M-2
	GRY-32	6.453	7.982	2.940	17.375	18.657	5.072	0.118	23.847	M-2
	GRY-43	5.522	7.846	3.075	16.443	16.578	4.845	0.126	21.549	M-3
GTD1	GTD-1	3.490	6.282	1.511	11.283	9.114	4.512	0.061	13.687	M-1
	GTD-2	3.492	6.767	2.032	12.292	9.392	4.903	0.078	14.374	M-1
	GTD-3	2.903	3.806	1.321	8.029	7.812	2.559	0.052	10.424	S-3
	GTD-4	2.091	3.598	1.726	7.415	6.013	2.157	0.069	8.239	S-3
	GTD-5	3.474	4.577	1.275	9.327	9.082	3.522	0.049	12.653	S-3
	GTD-6	2.842	5.134	1.813	9.790	7.665	3.676	0.073	11.414	S-3

surface area account for about 80% of the total pore volume and 95% of the total specific surface area, respectively (Table 2, Figures 8(b) and 8(c)).

5. Discussion

5.1. Relationship between Shale Mineral Composition and Pore Development. According to the results of CO_2 and N_2 adsorption, the parameters of micropores, mesopores, and macropores are shown in Table 2. For Devonian shale (well GTD1), TOC has a certain correlation with the total pore volume, indicating that TOC has an obvious contribution to the pore volume of Devonian shale (Figure 9(a)). TOC has strong correlation with micropores and mesopores and weak correlation with macropores, indicating that TOC mainly affects the development of micropores and mesopores (Figures 9(b)–9(d)). Meanwhile, the pore volume of Devonian shale (including micropores, mesopores, and macropores) is slightly negatively correlated with siliceous minerals and clay minerals (Figures 9(i)–9(l) and 9(m)–9(p)). However, the increase of micropore and mesopore volume related to organic matter is significantly greater than the decrease of micropore and mesopore volume related to siliceous minerals and clay minerals. It is worth mentioning that there is a weak positive correlation between Devonian shale carbonate minerals and pore volume (Figures 9(i)–9(l)). This weak positive correlation shows that carbonate minerals have a small contribution to the development of Devonian and Carboniferous shale pores. The specific reason may be that many dissolution pores are generated under the influence of dissolution, and these dissolution pores can also be seen under a scanning electron microscope (Figure 4(k)).

For Carboniferous shale (well GRY1), the correlation between TOC and total pore volume is not obvious, but TOC has strong correlation with micropore and mesopore volume and weak correlation with macropore, indicating that TOC has a certain contribution to the micropore and mesopore volume of Carboniferous shale (Figures 9(a) and 9(c)). At the same time, there is also an obvious positive correlation between clay minerals and total pore volume. Clay minerals have strong correlation with mesopores and macropores and weak correlation with micropores, indicating that clay minerals mainly affect the development of mesopores and macropores of Carboniferous shale (Figure 9(o)). However, due to the decrease of macropore volume related to TOC, siliceous minerals and carbonate minerals are greater than the increase of macropore volume related to clay minerals. Clay minerals have little effect on macropore volume, which is consistent with the adsorption test. Therefore, micropores and mesopores are the main components of the total pore volume in Carboniferous shale, accounting for 32.2% and 48.1%, respectively (Table 2, Figure 10). Meanwhile, it is worth mentioning that there is a weak positive correlation between Carboniferous shale carbonate minerals and pore volume, which may be related to the dissolution pores produced by the dissolution of carbonate minerals (Figure 4(i)).

For Devonian shale (well GTD1), TOC has a certain correlation with total pore volume, while clay minerals have a negative correlation with total pore volume. In Carboniferous shales, there is a good correlation between clay minerals and total pore volume. Therefore, there is a certain difference in the total pore volume between Devonian shale and Carboniferous shale, with an average of 9.7×10^{-3} cm^3/g and 17.3×10^{-3} cm^3/g, respectively. In addition, it is worth noting that the trend of specific surface area (including micropores, mesopores, and macropores) is similar to that of pore volume (Figure 11). The average specific surface areas of Devonian shale and Carboniferous shale are 11.8 m^2/g and 19.8 m^2/g, respectively (Table 2, Figure 10). This phenomenon may be due to the lower TOC and smaller micropore and mesopore volume of Devonian shale. Therefore, the pore volume of Carboniferous shale is also mainly provided by micropores and mesopores, accounting for 32% and 48% of the total pore volume, respectively (Table 2, Figure 10).

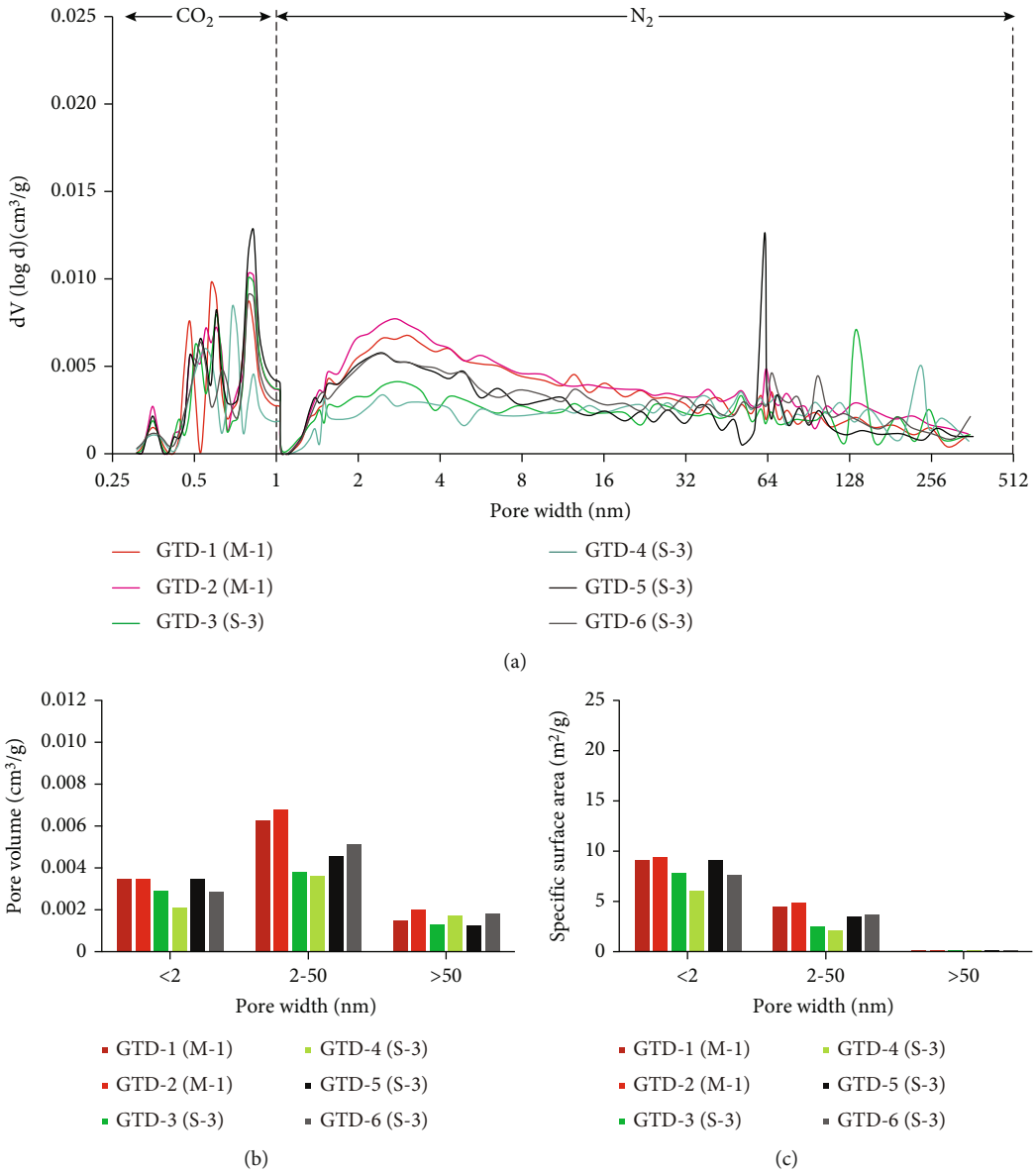

Figure 8: (a) N_2 and CO_2 pore diameter adsorption curve of Devonian shale samples in well GTD1; (b) pore volume distribution of Devonian shale samples in well GTD1; (c) pore specific surface area of Devonian shale samples in well GTD1.

Through the correlation analysis between TOC and mineral composition and both pore volume and specific surface area, we noted that although Devonian and Carboniferous shales have similar mineral composition and pore volume/specific surface area percentage distribution (Tables 1 and 2, Figure 10), there are obvious differences in the correlation between both pore volume and specific surface area and TOC and mineral composition. There is a certain correlation between TOC and pore volume of Devonian shale, which is obviously different from that of Carboniferous shale. The same is true for the relationship between TOC and pore specific surface area. In addition, there are significant differences in the relationship between clay minerals and pore volume or specific surface area between Devonian shale and Carboniferous shale. The clay minerals of Devonian shale have a significant negative correlation with pore volume or specific surface area. There is an obvious positive correlation between Carboniferous shale clay minerals and pore volume or specific surface area. This shows that TOC and mineral composition are not the main factors controlling the pore development of Devonian and Carboniferous shale.

5.2. Effect of Thermal Evolution (Ro) on Shale Pore Development. Previous studies have shown that the pore characteristics of organic-rich shale are mainly affected by sedimentary environment, mineral composition, organic matter type, thermal evolution, and tectonic movement [14, 25, 49]. Devonian and Carboniferous shales were formed in the platform-margin to open-platform

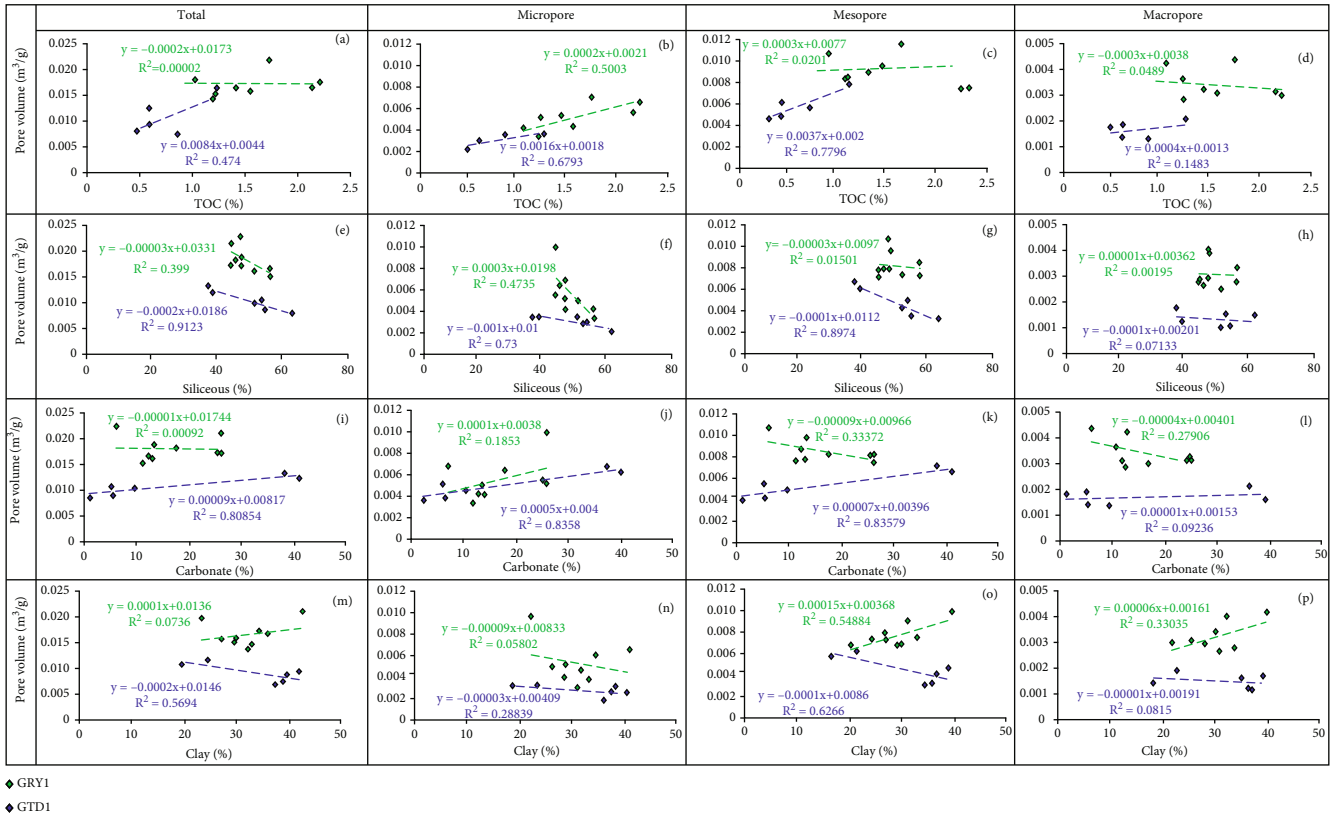

Figure 9: Correlation between shale material composition and pore volume.

sedimentary environment, with similar sedimentary environment and mineral composition, rich in organic matter and brittle minerals. However, the thermal evolution of Devonian and Carboniferous shale is different (Figure 12), which explains the difference (number and morphology) of organic pores between Devonian shale and Carboniferous shale in FE-SEM photos to a certain extent.

The contour map of regional thermal evolution shows that the thermal evolution of Carboniferous shale gradually decreases from northwest to Southeast (Figure 12(a)). The Ro of Carboniferous Luzhai shale in well GRY1 is about 2.0%, which is in a high maturity stage. At this stage, kerogen cracking degree is large, and organic matter begins to generate a large number of organic pores. In addition, it is worth mentioning that the asphalt components in shale at high maturity stage will also be cracked to form organic pores. Under the SEM, a large number of organic pores can be observed in the Carboniferous shale, and the pore morphology is mainly oval and circular (Figures 4(a), 4(b), 4(e), and 4(f)).

The thermal evolution of Devonian shale also decreases gradually from northwest to Southeast regionally (Figure 12(b)). The Ro of Luofu shale in well GTD1 is about 3.5%, which is in the overmature stage. After strong aromatization and polycondensation, kerogen tends to form graphite containing only carbon elements, which has a strong destructive effect on the previously formed organic pores. Under the SEM, Devonian shale also reflects the destruction of organic pores by too high thermal maturity. The number of organic pores in the electron microscope photos is less, and a small number of organic pores that can be observed also show the characteristics of merger and collapse (Figures 4(c), 4(d), 4(g), and 4(h)).

5.3. Control of Tectonic Preservation Conditions on Shale Pore Development. Tectonic preservation condition is one of the key factors for shale gas accumulation and release, and the development of fractures has two effects on shale gas-bearing property: (1) an appropriate amount of microfracture development can connect the pores of shale, increase the reservoir space and seepage capacity of shale, and improve the gas-bearing property of shale; (2) excessive fractures will destroy the existing sealing conditions of shale, cause the release of shale gas, and is unfavorable to the preservation of shale gas [23, 25].

The core can most intuitively and truly reflect the appearance of underground strata, through the statistical arrangement of the types and numbers of fractures in Carboniferous shale (well GRY1) and Devonian shale (well GTD1). Two main types of fractures in this area are bedding fractures and tectonic fractures, and the dip angle is generally less than 30°. However, there are great differences in fractures development characteristics between Carboniferous shale and Devonian shale (Figures 13 and 14).

There are relatively few fractures in Carboniferous shale (well GRY1), with a total of 2553 fractures, including 2392 bedding fractures and 161 tectonic fractures (Table 3, Figure 15).

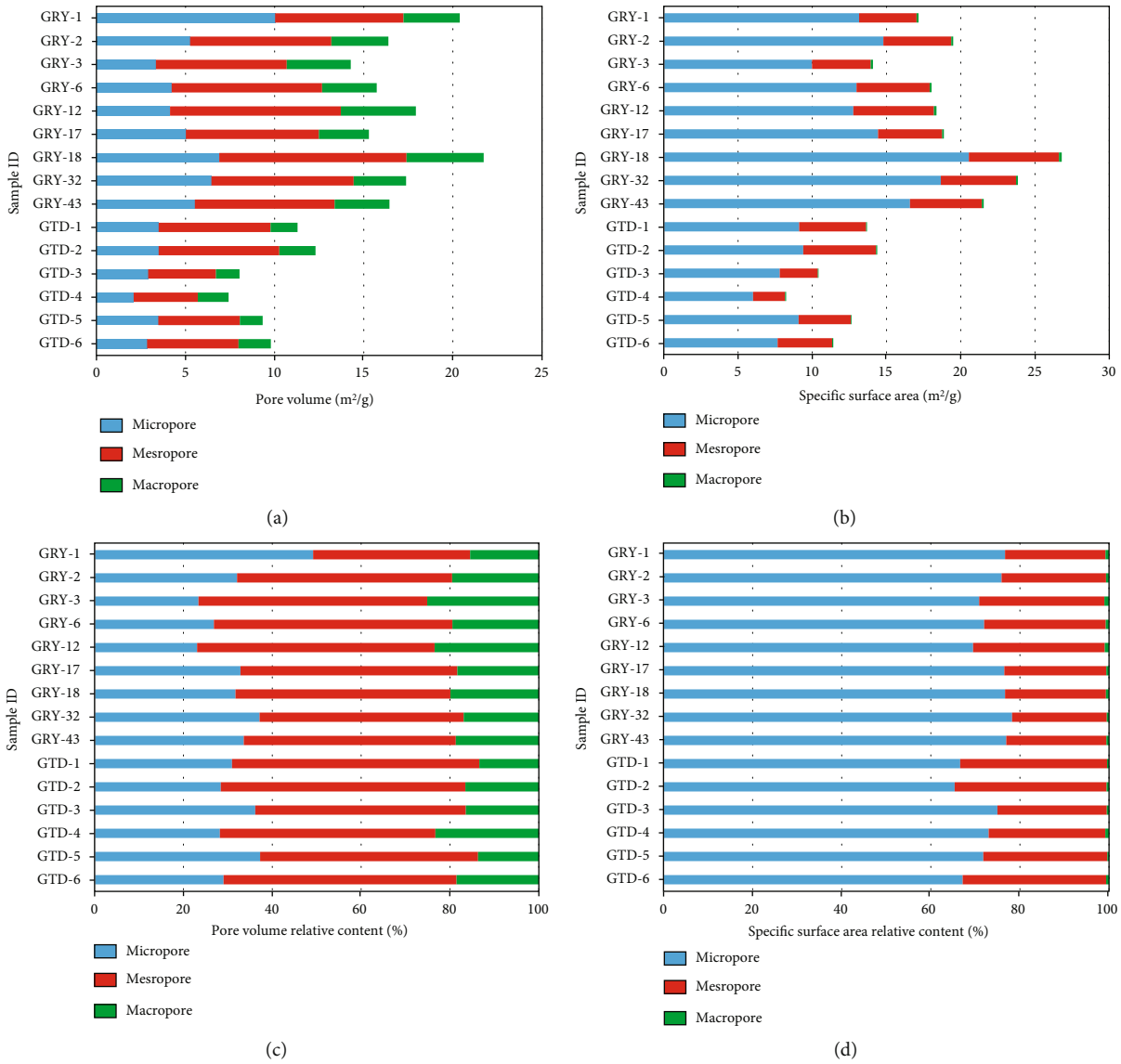

FIGURE 10: Pore volume and specific surface area and their percentage distribution in Devonian shale (well GTD1) and Carboniferous shale (well GRY1).

According to the type of fracture development, core can be divided into two sections. In the lower section, core is dominated by tectonic fractures, and a small amount of calcite veins, structural deformation, and bedding fractures can also be observed locally (Figures 13(a)–13(d)). It is revealed that the tectonic activity is relatively strong during sedimentary period [50, 51]. In the upper section, many bedding fractures and a few high angle tectonic fractures can be observed (Figures 13(e)–13(h)), indicating that the tectonic movement has tended to be stable and weak during sedimentation. A total of 7600 fractures are developed in the core of Devonian shale (well GTD1), including 1039 bedding fractures and 6561 tectonic fractures (Table 3, Figure 15). Core can also be further divided into three sections according to the development of fractures and calcite veins. Tectonic fractures are mainly developed in the lower section, with few bedding fractures; high-angle tectonic fractures filled with calcite are occasionally observed (Figures 14(a)–14(d)). A fault belt is encountered in the middle section, the core is relatively broken, and a large number of calcite veins and tectonic fractures are developed (Figures 14(e) and 14(f)). The development of calcite veins in the upper section is similar to that in the lower section, but there are more bedding fractures (Figures 14(g) and 14(h)), indicating that the tectonic activity is relatively stable during deposition [50, 51].

As mentioned above, many tectonic fractures and calcite veins are developed in Devonian shale; tectonic fractures account for 86% of the total fractures, which is significantly different from the fracture development characteristics in Carboniferous shale (mainly bedding fractures, accounting for 94% of the total fractures) (Table 3). This difference may be due to the fact that well

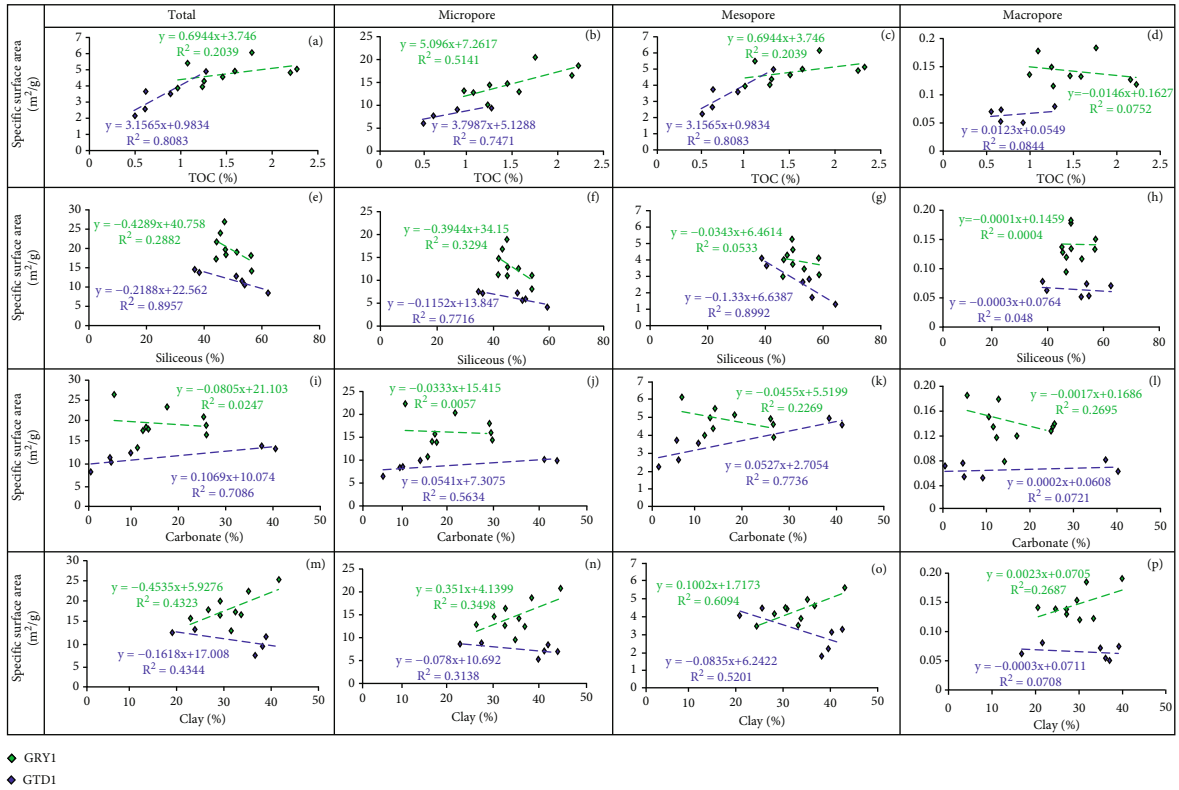

Figure 11: Correlation between shale material composition and specific surface area.

GTD1 is close to the fault belt and affected by tectonism obviously. Too many tectonic fractures will reduce the shale reservoir pressure, making it difficult to preserve organic pores under compaction [36, 45, 49, 52, 53]. This is consistent with the observation of a scanning electron microscope.

Under the electron microscope, there are obvious differences in the number and morphology of organic pores between Carboniferous shale and Devonian shale. The organic pores of Carboniferous shale (well GRY1) are relatively developed, the pore shape is circular elliptical, and long strips in directional arrangement are occasionally seen (Figure 16(a)). Devonian shale (well GTD1) has few organic pores, and most of them have been closed (Figure 16(b)). The development of organic pores can only be observed in a few organic matter. Due to the high thermal evolution, the organic pores are merged, and the pore morphology presents irregular characteristics, mainly flat or angular (Figure 16(b)).

There are also many differences in pore structure between Carboniferous shale and Devonian shale. FE-SEM images are processed by JMicroVision (Figure 17). The surface porosity of Carboniferous shale is mainly distributed between 2% and 9%, with an average of 6%. And the surface porosity of Devonian shale is mainly distributed between 0.2% and 26%, with an average of 9%. The surface porosity distribution among different Devonian shale samples is quite different, which may be related to the collapse and closure of organic pores in the samples (Figure 18).

Although Carboniferous shale and Devonian shale have similar pore size distribution, Devonian shale has fewer organic pores, lower surface porosity, and smaller pore volume and specific surface area than Carboniferous shale. This phenomenon may also be due to the fact that well GTD1 is affected by tectonic movement [11, 25, 34, 54, 55]. Meanwhile, tectonic fractures and calcite veins are well developed in the core of Devonian shale (well GTD1). Therefore, the Devonian shale of well GTD1 has poor preservation conditions and high hydrocarbon expulsion efficiency. The result is that many organic pores in Devonian shale are compressed or closed under the compaction of overlying strata, the pore shape is flat or angular, and the roundness is low.

Therefore, although shale has similar or identical lithofacies, the fracture development and pore characteristics of shale may also be different. As mentioned above, due to strong tectonic deformation, tectonic fractures are mainly developed in Devonian shale, and bedding fractures are relatively less developed. A large number of tectonic fractures lead to poor sealing conditions of shale and serious release of shale gas. With the release of shale reservoir pressure, organic pores collapse or even close (Figures 16(e) and 16(f)). Therefore, the influence of tectonic preservation conditions on the pore volume and specific surface area is very huge. The pore volume and specific surface area of Carboniferous shale are 78.3% and 67.8% higher than Devonian shale, respectively.

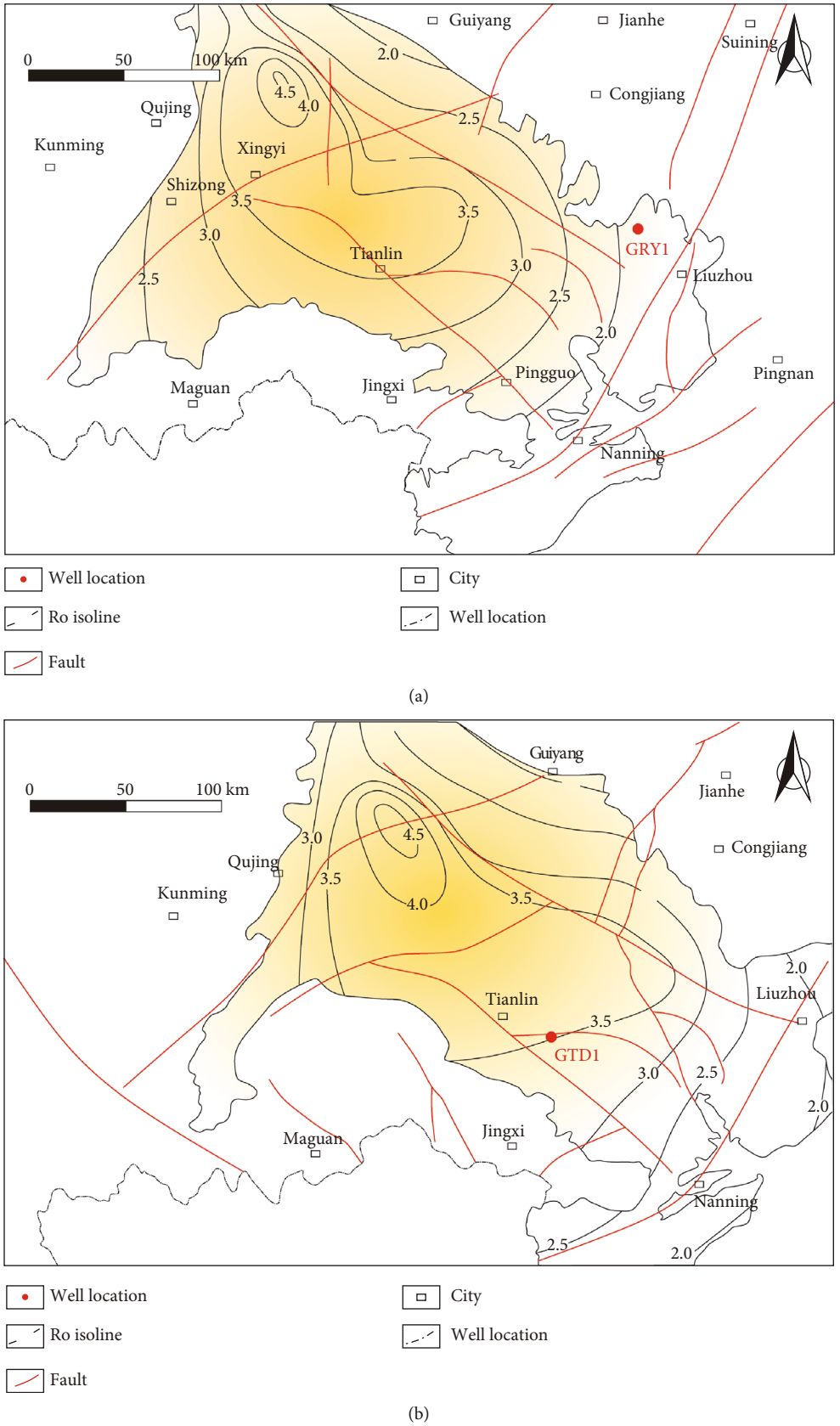

Figure 12: (a) Ro contour map of organic rich shale of Lower Carboniferous Luzhai formation; (b) Ro contour map of organic rich shale of Middle Devonian Luofu formation.

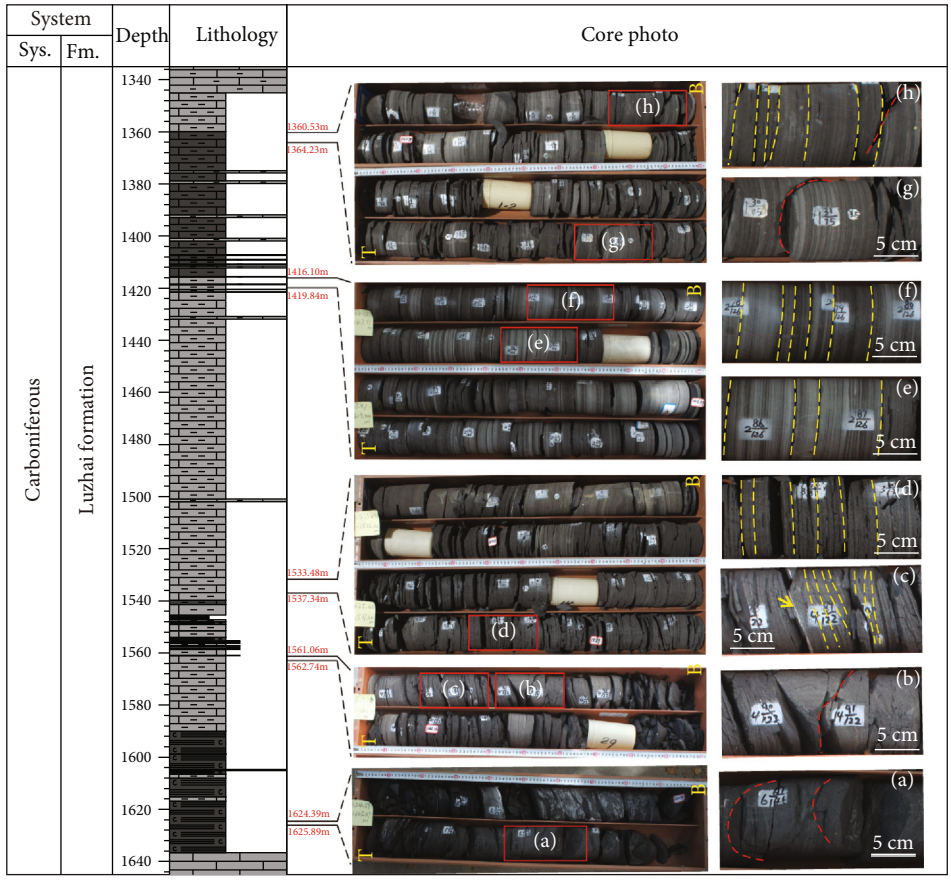

Figure 13: Typical core photos of Lower Carboniferous Luzhai organic-rich shale in well GRY1.

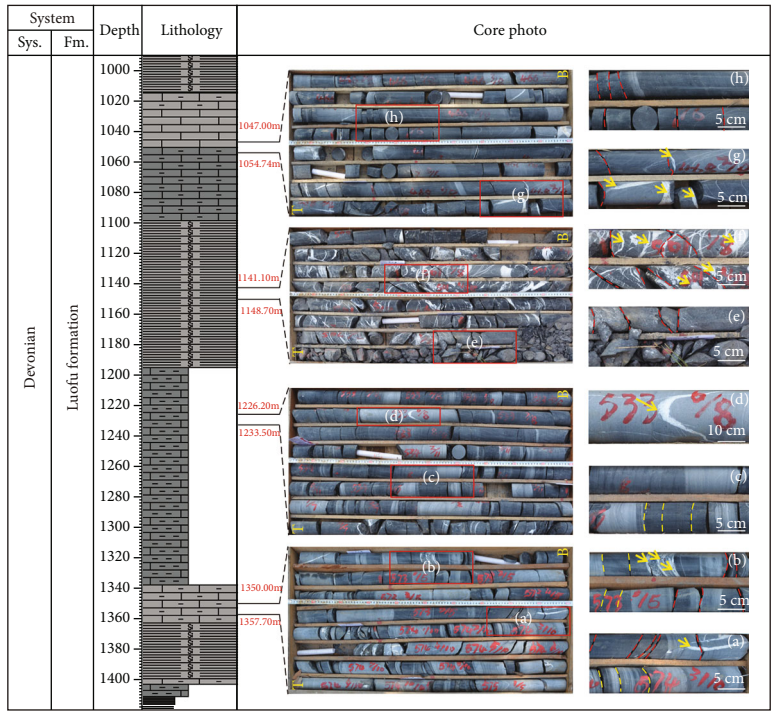

Figure 14: Typical core photos of Middle Devonian Luofu organic-rich shale in well GTD1.

Table 3: Statistical results of fracture types and numbers of GRY1 and GTD1.

Well	Bedding fractures		Tectonic fracture		Total
	Number	Percentage	Number	Percentage	
GRY1	2392	94%	161	6%	2553
GTD1	1039	14%	6561	86%	7600

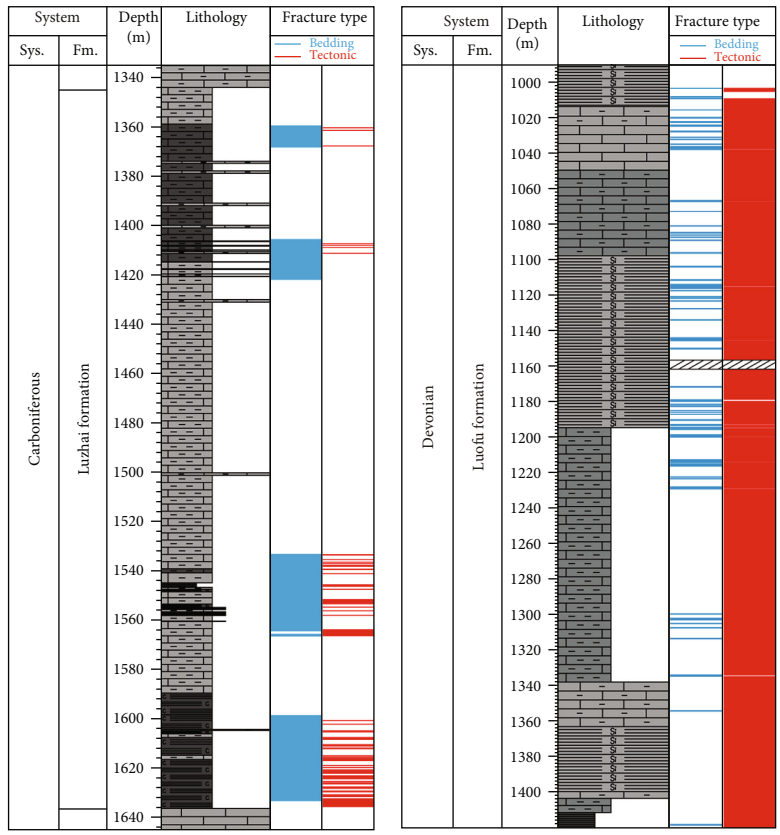

Figure 15: (a) Statistical results of fracture type and development in Carboniferous shale (well GRY1); (b) statistical results of fracture type and development in Devonian shale (well GTD1).

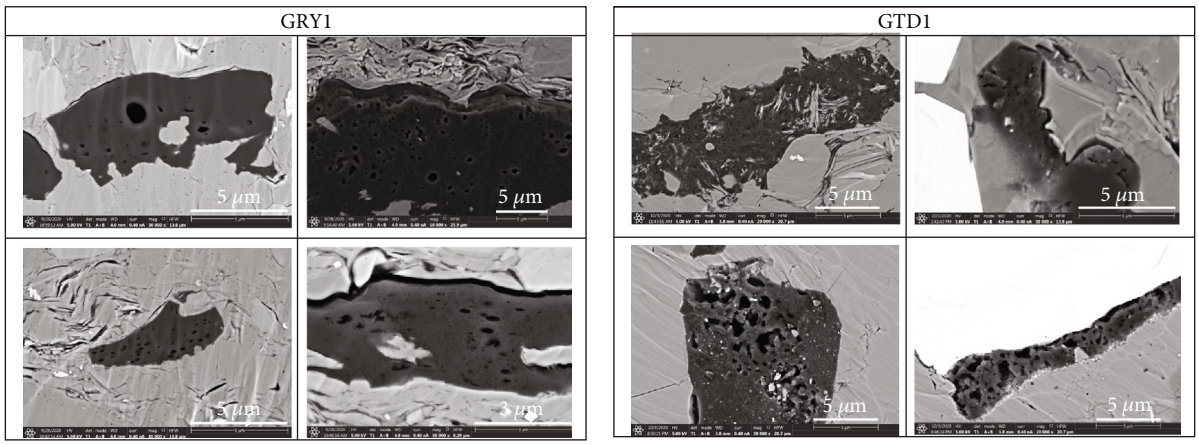

Figure 16: (a) Typical SEM photos of organic pores in Carboniferous shales (well GRY1); (b) typical SEM photos of organic pores in Devonian shales (well GTD1).

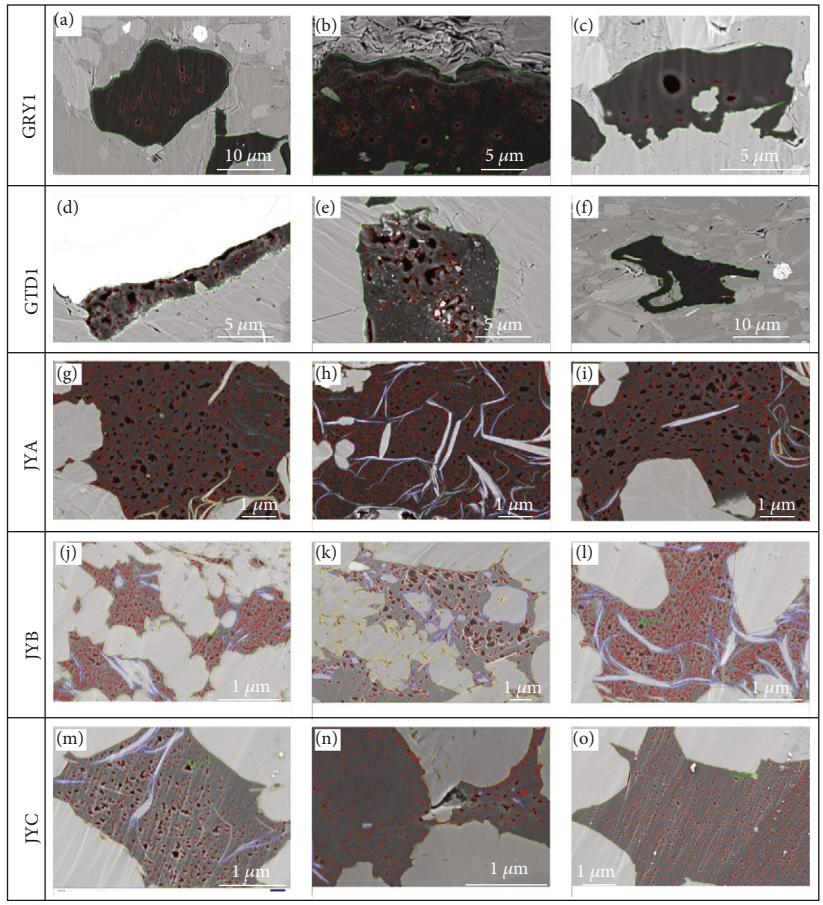

Figure 17: SEM photos of surface porosity identification in the study area and Jiaoshiba area.

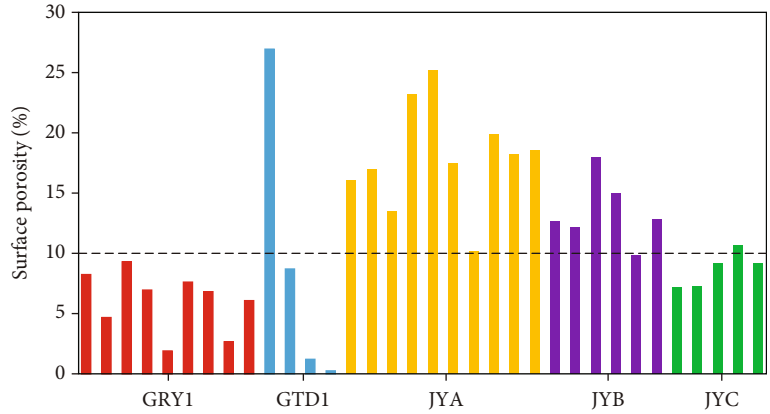

Figure 18: Surface porosity of shale samples in the study area and Jiaoshiba area.

6. Conclusions

(1) According to the XRD results, the Devonian and Carboniferous shales in the study area have similar mineral characteristics, which are dominated by siliceous minerals, ranging from 44.1% to 62.1% (average 48%), followed by clay minerals, ranging from 18.2% to 41.1% (average 31%), and carbonate minerals are the least, ranging from 0.5% to 40.3% (average 17%). Meanwhile, four lithofacies are developed in the two sets of shale strata: mixed shale (M), carbonate/siliceous mixed shale (M-1), argillaceous/siliceous mixed shale (M-2), and argillaceous-rich siliceous shale (S-3)

(2) The pore types of Devonian and Carboniferous shale samples in the study area mainly are organic pores, inorganic pores, and microfractures. All three types of pores are developed in Carboniferous shale, and organic pores are mainly round oval, and a small part is slit or strip. Inorganic pores and microfractures are mainly developed in Devonian shale; a few developed organic pores show the characteristics of collapse and closure. Meanwhile, there are also obvious differences in pore structures between Carboniferous shale and Devonian shale. The average total pore volume and specific surface area of Devonian shale are $9.7 \times 10^{-3}\,cm^3/g$ and $11.8\,m^2/g$, respectively, which are 78.3% and 67.8% lower than those of Carboniferous shale

(3) Thermal evolution (Ro) affected the pore development of Devonian and Carboniferous shale. The Ro of Carboniferous shale is about 2%, which is in the stage where organic matter begins to produce a large number of organic pores. The Ro of Devonian shale is about 3.5%. Too high thermal evolution has a strong destructive effect on the previously formed organic pores, which is not conducive to the preservation of organic pores

(4) Tectonic preservation conditions controlled the pore development of Devonian and Carboniferous shale. The Carboniferous shale (well GRY1) has better tectonic preservation conditions and is conducive to the preservation of organic pores. The Devonian shale (well GTD1) is strongly affected by tectonic movement, it is difficult to maintain formation pressure under sealing conditions, and organic pores are deformed or even closed under compaction

Data Availability

The data used to support the findings of this study are included in the article.

Conflicts of Interest

The authors declare that they have no conflicts of interest.

Acknowledgments

This research was supported by the National Natural Science Foundation of China (42122017, 41821002), the Shandong Provincial Key Research and Development Program (2020ZLYS08), and the Independent innovation research program of China University of Petroleum (East China) (21CX06001A).

References

[1] J. R. Fanchi, M. J. Cooksey, K. M. Lehman, A. Smith, A. C. Fanchi, and C. J. Fanchi, "Probabilistic decline curve analysis of Barnett, Fayetteville, Haynesville, and Woodford gas shales," *Journal of Petroleum Science & Engineering*, vol. 109, pp. 308–311, 2013.

[2] Z. Gao, H. Zheng, and H. Tao, "Attributes of sweet spots in the Devonian Woodford shales in Oklahoma, USA," *Petroleum Geology & Experiment*, vol. 38, no. 3, pp. 340–345, 2016.

[3] M. G. Kibria, Q. Hu, H. Liu, Y. Zhang, and J. Kang, "Pore structure, wettability, and spontaneous imbibition of Woodford Shale, Permian Basin, West Texas," *Marine and Petroleum Geology*, vol. 91, pp. 735–748, 2018.

[4] R. J. Hill, E. Zhang, B. J. Katz, and Y. Tang, "Modeling of gas generation from the Barnett Shale, Fort Worth Basin, Texas," *AAPG Bulletin*, vol. 91, no. 4, pp. 501–521, 2007.

[5] B. Fairhurst, T. Ewing, and B. Lindsay, "West Texas (Permian) Super Basin, United States: tectonics, structural development, sedimentation, petroleum systems, and hydrocarbon reserves," *AAPG Bulletin*, vol. 105, no. 6, pp. 1099–1147, 2021.

[6] D. Jarvie, R. Hill, T. Ruble, and R. M. Pollastro, "Unconventional shale-gas systems: the Mississippian Barnett Shale of north-central Texas as one model for thermogenic shale-gas assessment," *AAPG Bulletin*, vol. 91, no. 4, pp. 475–499, 2007.

[7] F. Hao, H. Zou, and Y. Lu, "Mechanisms of shale gas storage: implications for shale gas exploration in China," *AAPG Bulletin*, vol. 97, no. 8, pp. 1325–1346, 2013.

[8] B. Bruns, R. Littke, M. Gasparik, J. D. V. Wees, and S. Nelskamp, "Thermal evolution and shale gas potential estimation of the Wealden and Posidonia shale in NW-Germany and the Netherlands: a 3D basin modelling study," *Basin Research*, vol. 28, no. 1, pp. 2–33, 2016.

[9] Q. Gou, S. Xu, F. Hao et al., "Characterization method of shale pore structure based on nano-CT: a case study of Well JY-1," *Acta Petrolei Sinica*, vol. 39, no. 11, pp. 1253–1261, 2018.

[10] Q. Gou and S. Xu, "Quantitative evaluation of free gas and adsorbed gas content of Wufeng-Longmaxi shales in the Jiaoshiba area, Sichuan Basin, China," *Advances in Geo-Energy Research*, vol. 3, no. 3, pp. 258–267, 2019.

[11] Q. Gou, S. Xu, F. Hao et al., "Full-scale pores and microfractures characterization using FE-SEM, gas adsorption, nano-CT and micro-CT: a case study of the Silurian Longmaxi Formation shale in the Fuling area, Sichuan Basin, China," *Fuel*, vol. 253, pp. 167–179, 2019.

[12] Y. Ma, Y. Lu, X. Liu, G. Zhai, Y. Wang, and C. Zhang, "Depositional environment and organic matter enrichment of the lower Cambrian Niutitang shale in western Hubei Province, South China," *Marine and Petroleum Geology*, vol. 109, pp. 381–393, 2019.

[13] J. Li, Z. Li, C. Zhang, H. Cui, and Z. Zhu, "Characteristics and genetic types of the Lower Paleozoic natural gas, Ordos Basin," *Marine & Petroleum Geology*, vol. 89, pp. 106–119, 2018.

[14] R. G. Loucks, R. M. Reed, S. C. Ruppel, and U. Hammes, "Spectrum of pore types and networks in mudrocks and a descriptive classification for matrix-related mudrock pores," *AAPG Bulletin*, vol. 96, no. 6, pp. 1071–1098, 2012.

[15] M. Mastalerz, A. Schimmelmann, A. Drobniak, and Y. Chen, "Porosity of Devonian and Mississippian New Albany Shale across a maturation gradient: insights from organic petrology, gas adsorption, and mercury intrusion," *AAPG Bulletin*, vol. 97, no. 10, pp. 1621–1643, 2013.

[16] F. Yang, Z. Ning, Q. Wang, R. Zhang, and B. M. Krooss, "Pore structure characteristics of lower Silurian shales in the southern Sichuan Basin, China: insights to pore development and gas storage mechanism," *International Journal of Coal Geology*, vol. 156, pp. 12–24, 2016.

[17] L. Chen, Z. Jiang, K. Liu, J. Tan, F. Gao, and P. Wang, "Pore structure characterization for organic-rich Lower Silurian shale in the Upper Yangtze Platform, South China: a possible mechanism for pore development," *Journal of Natural Gas Science and Engineering*, vol. 46, pp. 1–15, 2017.

[18] A. Li, W. Ding, K. Jiu, Z. Wang, R. Wang, and J. He, "Investigation of the pore structures and fractal characteristics of marine shale reservoirs using NMR experiments and image analyses: a case study of the Lower Cambrian Niutitang Formation in northern Guizhou Province, South China," *Marine and Petroleum Geology*, vol. 89, pp. 530–540, 2018.

[19] Y. Xia, J. Cai, W. Wei, X. Hu, X. Wang, and X. Ge, "A new method for calculating fractal dimensions of porous media based on pore size distribution," *Fractals*, vol. 26, no. 1, article 1850006, 2018.

[20] X. Zheng, B. Zhang, H. Sanei et al., "Pore structure characteristics and its effect on shale gas adsorption and desorption behavior," *Marine and Petroleum Geology*, vol. 100, pp. 165–178, 2019.

[21] R. Wang, Z. Hu, C. Sun et al., "Comparative analysis of shale reservoir characteristics in the Wufeng-Longmaxi (O3w-S1l) and Niutitang (∈1n) Formations: a case study of Wells JY1 and TX1 in the southeastern Sichuan Basin and its neighboring areas, southwestern China," *Interpretation*, vol. 6, no. 4, 2018.

[22] R. Wang, Z. Hu, S. Long et al., "Differential characteristics of the Upper Ordovician-Lower Silurian Wufeng- Longmaxi shale reservoir and its implications for exploration and development of shale gas in/around the Sichuan Basin," *Acta Geologica Sinica - English Edition*, vol. 93, no. 3, pp. 520–535, 2019.

[23] S. Xu, Q. Gou, F. Hao et al., "Shale pore structure characteristics of the high and low productivity wells, Jiaoshiba shale gas field, Sichuan Basin, China: dominated by lithofacies or preservation condition?," *Marine and Petroleum Geology*, vol. 114, article 104211, 2020.

[24] Z. Liu, G. Liu, Z. Hu et al., "Lithofacies types and assemblage features of continental shale strata and their significance for shale exploration: a case study of the Middle and Lower Jurassic strata in the Sichuan Basin," *Natural Gas Industry*, vol. 39, no. 12, pp. 10–21, 2019.

[25] K. Milliken, W. Esch, R. Reed, and T. Zhang, "Grain assemblages and strong diagenetic overprinting in siliceous mudrocks, Barnett Shale (Mississippian), Fort Worth basin, Texas," *AAPG Bulletin*, vol. 96, no. 8, pp. 1553–1578, 2012.

[26] L. Chen, Z. Jiang, K. Liu et al., "Effect of lithofacies on gas storage capacity of marine and continental shales in the Sichuan Basin, China," *Journal of Natural Gas Science and Engineering*, vol. 36, pp. 773–785, 2016.

[27] J. James and B. H. Hickey, "Lithofacies summary of the Mississippian Barnett shale, Mitchell 2 T.P. Sims well, wise county, Texas," *AAPG Bulletin*, vol. 91, no. 4, pp. 437–443, 2007.

[28] R. G. Loucks and S. C. Ruppel, "Mississippian Barnett shale: lithofacies and depositional setting of a deep-water shale-gas succession in the Fort Worth Basin, Texas," *AAPG Bulletin*, vol. 91, no. 4, pp. 579–601, 2007.

[29] M. O. Abouelresh and R. M. Slatt, "Lithofacies and sequence stratigraphy of the Barnett Shale in east-central Fort Worth Basin, Texas," *AAPG Bulletin*, vol. 96, no. 1, pp. 1–22, 2012.

[30] J. Mason, J. Carloni, S. Baker, A. Zehnder, and T. Jordan, "Dependence of micromechanical properties on lithofacies: indentation experiments on Marcellus Shale," in *Unconventional resources Technology conference (URTEC)*, Denver, Colorado, USA, 2014.

[31] D. J. K. Ross and R. M. Bustin, "The importance of shale composition and pore structure upon gas storage potential of shale gas reservoirs," *Marine and Petroleum Geology*, vol. 26, no. 6, pp. 916–927, 2009.

[32] G. R. Chalmers, R. M. Bustin, and I. M. Power, "Characterization of gas shale pore systems by porosimetry, pycnometry, surface area, and field emission scanning electron microscopy/transmission electron microscopy image analyses: examples from the Barnett, Woodford, Haynesville, Marcellus, and

Doig units," *AAPG Bulletin*, vol. 96, no. 6, pp. 1099–1119, 2012.

[33] J. Wang, X. Li, Z. Xu, Y. Xin, Z. Li, and Y. Li, "Shale gas accumulation conditions and favorable area prediction of Lower Carboniferous Luzhai Formation in Donglan area of Nanpanjiang Depression," *Earth Science*, vol. 46, no. 5, pp. 1814–1828, 2021.

[34] X. Guo, D. Hu, Y. Li, Z. Wei, X. Wei, and Z. Liu, "Geological factors controlling shale gas enrichment and high production in Fuling shale gas field," *Petroleum Exploration and Development*, vol. 44, no. 4, pp. 513–523, 2017.

[35] P. Wang, Z. Jiang, W. Ji et al., "Heterogeneity of intergranular, intraparticle and organic pores in Longmaxi shale in Sichuan Basin, South China: evidence from SEM digital images and fractal and multifractal geometries," *Marine and Petroleum Geology*, vol. 72, pp. 122–138, 2016.

[36] S. Xu, Q. Gou, F. Hao, B. Zhang, Z. Shu, and Y. Zhang, "Multiscale faults and fractures characterization and their effects on shale gas accumulation in the Jiaoshiba area, Sichuan Basin, China," *Journal of Petroleum Science and Engineering*, vol. 189, no. 189, article 107026, 2020.

[37] L. Qiu, D.-P. Yan, S.-L. Tang et al., "Mesozoic geology of southwestern China: Indosinian foreland overthrusting and subsequent deformation," *Journal of Asian Earth Sciences*, vol. 122, pp. 91–105, 2016.

[38] L. Qiu, D.-P. Yan, S.-L. Tang et al., "Insights into post-orogenic extension and opening of the Palaeo-Tethys Ocean recorded by an Early Devonian core complex in South China," *Journal of Geodynamics*, vol. 135, article 101708, 2020.

[39] X. Y. He, G. S. Yao, X. S. He et al., "Bitumen genesis and hydrocarbon accumulation pattern of Well Guizhong-1 in Guizhong Depression," *Acta Petrolei Sinica*, vol. 31, no. 3, 2010.

[40] K. M. Wang, "Shale gas accumulation conditions of Devonian strata in Guizhong depression," *Geology in China*, vol. 40, no. 2, pp. 403–438, 2013.

[41] Z. C. Mao, Y. S. Du, M. Zhang, J. X. Yan, and F. Zeng, "Organic geochemical characterization and depositional paleoenvironments of the Devonian strata in Guizhong region, Guangxi, China," *Science in China Series D: Earth Sciences*, vol. 52, no. S1, pp. 88–95, 2009.

[42] S. Luo, C. Wang, and Z. Peng, "Shale gas research of Luzhai Formation, Low Carboniferous in Guizhong Depression," *Geology and Mineral Resources of South China*, vol. 32, no. 2, pp. 180–190, 2016.

[43] B. Kya, A. Whh, C. Xxf et al., "Geochemical characteristics and sedimentary environment of the Middle Devonian organic-rich shales in the northwest of Guizhong Depression, Southwest China," *China Geology*, vol. 4, pp. 567–574, 2020.

[44] R. G. Loucks, R. M. Reed, S. C. Ruppel, and D. M. Jarvie, "Morphology, genesis, and distribution of nanometer-scale pores in siliceous mudstones of the Mississippian Barnett Shale," *Journal of Sedimentary Research*, vol. 79, no. 12, pp. 848–861, 2009.

[45] K. L. Milliken, M. Rudnicki, D. N. Awwiller, and T. Zhang, "Organic matter-hosted pore system, Marcellus Formation (Devonian), Pennsylvania," *AAPG Bulletin*, vol. 97, no. 2, pp. 177–200, 2013.

[46] C. Scherdel, G. Reichenauer, and M. Wiener, "Relationship between pore volumes and surface areas derived from the evaluation of N_2-sorption data by DR-, BET- and t-plot," *Microporous and Mesopores Materials*, vol. 132, no. 3, pp. 572–575, 2010.

[47] L. Wu, Y. Lu, S. Jiang, Y. Lu, X. Liu, and H. Hu, "Pore structure characterization of different lithofacies in marine shale: a case study of the Upper Ordovician Wufeng-Lower Silurian Longmaxi formation in the Sichuan Basin, SW China," *Journal of Natural Gas Science and Engineering*, vol. 57, pp. 203–215, 2018.

[48] X. Guo, Z. Qin, R. Yang et al., "Comparison of pore systems of clay-rich and silica-rich gas shales in the lower Silurian Longmaxi formation from the Jiaoshiba area in the eastern Sichuan Basin, China," *Marine and Petroleum Geology*, vol. 101, pp. 265–280, 2019.

[49] J. Zhao, Z. Jin, Q. Hu et al., "Mineral composition and seal condition implicated in pore structure development of organic-rich Longmaxi shales, Sichuan Basin, China," *Marine and Petroleum Geology*, vol. 98, pp. 507–522, 2018.

[50] Y. Gu, J. He, S. Xu, Q. Tian, W. Zhang, and S. Yin, "Influence of differential structural deformation on shale reservoirs: a case study of the lower Silurian Longmaxi Shale in north Guizhou, Southern China," *Geological Magazine*, vol. 158, no. 4, pp. 673–684, 2021.

[51] S. Li, Y. Li, Z. He, K. Chen, Y. Zhou, and D. Yan, "Differential deformation on two sides of Qiyueshan Fault along the eastern margin of Sichuan Basin, China, and its influence on shale gas preservation," *Marine and Petroleum Geology*, vol. 121, article 104602, 2020.

[52] J. Yi, H. Bao, A. Zheng et al., "Main factors controlling marine shale gas enrichment and high-yield wells in South China: a case study of the Fuling shale gas field," *Marine and Petroleum Geology*, vol. 103, pp. 114–125, 2019.

[53] Z. Jin, H. Nie, Q. Liu, J. Zhao, and T. Jiang, "Source and seal coupling mechanism for shale gas enrichment in upper Ordovician Wufeng Formation - Lower Silurian Longmaxi Formation in Sichuan Basin and its periphery," *Marine and Petroleum Geology*, vol. 97, pp. 78–93, 2018.

[54] D. Hu, H. Zhang, K. Ni, and G. C. Yu, "Main controlling factors for gas preservation conditions of marine shales in southeastern margins of the Sichuan Basin," *Natural Gas Industry*, vol. 34, no. 6, pp. 17–23, 2014.

[55] X. She, J. Chen, S. Zhang et al., "Tectonic characteristics and their shale gas geological significance of the Mesozoic-Paleozoic in Jiaoshiba area, the Sichuan Basin," *Oil and Gas Geology*, vol. 37, no. 6, pp. 828–837, 2016.